Scientia Horticulturae 360 (2026) 114741

Contents lists available at ScienceDirect

Scientia Horticulturae

journal homepage: www.elsevier.com/locate/scihorti

Research Paper

Precision breeding for drought tolerance using a Copeland method: Integrating receiver operating characteristic analysis and multi-criteria decision making to identify superior Persian walnut genotypes

Asaad Habibi [a], Mohammad Soltani [b], Saadat Sarikhani [a,*], Mahmoud Reza Roozban [a], Adamo Domenico Rombolà [c], Mohammad Hassan Jafari Sayadi [d], Kourosh Vahdati [a,*]

[a] Department of Horticulture, College of Aburaihan, University of Tehran, Tehran, Iran
[b] Independent Researcher in the Field of Water Resources Engineering, Iran
[c] Department of Agricultural and Food Sciences, University of Bologna, Italy
[d] Department of Agriculture and Natural Resources, Payam Noor University, Tehran, Iran

ARTICLE INFO

Keywords:
Germplasm evaluation
ROC curve analysis
Path analysis
Walnut tree breeding
Genetic resources
Phenotypic variation

ABSTRACT

The scarcity of drought-tolerant rootstocks threatens the sustainability of walnut (*Juglans regia* L.) production, given the crop's high-water requirements and sensitivity to drought. Selecting a drought-tolerant genotype is a critical challenge due to the broad impact of drought on various traits, which requires evaluating multiple, unequally weighted criteria, making it a complex multi-criteria decision-making (MCDM) problem. This study investigates the genetic and phenotypic diversity of 183 walnut genotypes, originating from seven regions of Iran with diverse climatic conditions, which were subjected to severe drought stress (DS) in a common garden approach. DS was applied by water withholding for a 30-day period, and various phenotypic, physiological, and biochemical traits were assessed at the end of the period. The results revealed that drought-tolerant genotypes exhibited higher tolerance indices, with less reduction in RWC, MSI, and photosynthetic pigments, along with decreased wilting and leaf shedding. Moreover, these genotypes demonstrated significantly higher antioxidant enzyme activity, osmotic regulation, and photosynthetic efficiency compared to sensitive ones. The receiver operating characteristic (ROC) curve-plotting algorithm, based on the criteria of area under the curve (AUC) and Youden index (YI), highlighted the superior discrimination ability of specific indices between susceptible and tolerant genotypes and determined the optimal thresholds (OT) for the measured traits. Among the characteristics, FV/FM (AUC: 0.9965, YI: 0.9669, OT: 0.6365), PIABS (AUC: 0.9961, YI: 0.9556, OT: 0.89), TChl (AUC: 0.9915, YI: 0.9158, OT: 2527), carotenoids (AUC: 0.9892, YI: 0.9139, OT: 708), and RWC (AUC: 0.9739, YI: 0.9026, OT: 62.7 screening key indices, respectively. To identify superior genotypes, a proposed framework was employed, utilizing the ROC approach to weight the measured traits, followed by the application of four prominent MCDM methods, including VIKOR, TOPSIS, SAW, and ELECTRE, integrated with a Copeland ranking aggregation technique to achieve a consensus-based final ranking of genotypes. Based on the aggregated Copeland results, the genotypes Ke16, KeSH9, and Ke18 were identified as the superior drought-tolerant genotypes. It can be concluded that the application of MCDM methods and the Copeland aggregation approach provides breeders with a powerful tool to select superior genotypes for developing drought-tolerant cultivars with high precision and efficiency.

1. Introduction

The Iranian Plateau is one of the main centers of walnut (*Juglans regia* L) diversity and domestication (Hassani et al., 2020; Habibi et al., 2022). Native populations are widespread across diverse climates, thriving in areas where temperatures range from -9 to +30°C and annual rainfall during growth varies between 175 and 1150 mm (Vahdati et al., 2023; Momayyezi et al., 2022). Extensive sexual propagation, cross-pollination, and dichogamy have fostered high genetic diversity in both wild and cultivated walnuts (Kouhi et al., 2020; Taheri et al.,

* Corresponding authors.
E-mail addresses: saadat.sarikhani@ut.ac.ir (S. Sarikhani), kvahdati@ut.ac.ir (K. Vahdati).

https://doi.org/10.1016/j.scienta.2026.114741
Received 21 October 2025; Received in revised form 27 February 2026; Accepted 3 March 2026
Available online 13 April 2026

2026). Consequently, Iranian walnuts exhibit considerable trait variability and are well-adapted to diverse climates, making them valuable for breeding programs through selection or hybridization (Vahdati et al., 2019).

The primary objective in walnut cultivation is to develop rootstocks, particularly those compatible with Persian walnut varieties and resilient to abiotic stresses, which highlights the urgent need to exploit new genetic resources (Habibi et al., 2025). Wild germplasm collections in Iran can serve as a valuable source for increasing genetic diversity aimed at improving tolerance to biotic and abiotic stresses and enhancing crop productivity (Vahdati et al., 2021). Nevertheless, to date, this collection has not been utilized for identifying genotypes with higher tolerance to abiotic stresses and physiological traits related to improved performance.

In *Juglans regia* L., genetic variation in response to drought stress (DS) among different genotypes mainly arises from structural, physiological, and biochemical differences in the leaves. These differences are closely associated with the climatic conditions of their native habitats, particularly latitude, temperature, precipitation patterns, and length of the growing season (Arab et al., 2020; Momayyezi et al., 2022). These inherent leaf traits, together with regulatory mechanisms related to photosynthesis, water balance, osmotic regulators, and enzymatic responses, play a key role in determining the level of drought tolerance of each genotype (Arab et al., 2023; Momayyezi et al., 2025). Therefore, this intraspecific variation can serve as a valuable resource in breeding programs aimed at identifying and selecting superior genotypes with optimal performance under water-limited conditions.

Climate change has increasingly altered the environmental conditions under which walnut trees grow, with significant implications for their phenology, distribution, and productivity (Chatrabnous et al., 2024). Rising global temperatures have been linked to shifts in phenological events, such as earlier onset of flowering and leaf emergence, which can increase vulnerability to late frost damage and extend the growing season, thereby exacerbating water demand and drought exposure in walnut orchards (Xu et al., 2018; Habibi et al., 2025). Climate models also indicate that changes in temperature and precipitation regimes are likely to influence the geographical distribution of suitable walnut habitats, potentially expanding cultivation zones in some regions while introducing stress in others due to heat and moisture imbalance (Robin et al., 2024; Farajpour, 2025a). Moreover, walnut growth responses along elevational and climatic gradients reveal that temperature remains a critical driver of radial growth, and extreme weather variability can modify the sensitivity of growth to water availability (Xu et al., 2018). These climate-driven changes in environmental patterns including warmer winters, more frequent heat stress events, and altered rainfall are increasingly recognized as key factors shaping walnut tree performance, stressing the need for adaptive management and breeding strategies to sustain productivity under future climate scenarios.

Drought stress affects various aspects of plant growth and development by causing morphological, physiological, photosynthetic, and biochemical changes, and these changes are evident in all phenological stages of the plant, at any stage where water deficiency occurs (Momayyezi et al., 2025). The response to DS includes a decrease in photosynthesis, a decrease in leaf expansion, stomatal closure, disruption of the photosynthetic apparatus, increased production of reactive oxygen species (ROS), premature leaf senescence, a decrease in assimilate transport, and a decrease in yield (Habibi et al., 2024; Momayyezi et al., 2025). Therefore, plants are forced to develop a wide range of reactions or mechanisms at the physiological, biochemical, and molecular levels to survive under DS conditions to adapt and adapt to environmental conditions (Arab et al., 2020; Habibi et al., 2025).

The increasing frequency and intensity of drought events under ongoing climate change, coupled with the inherently high-water requirements of most commercial walnut cultivars, have emerged as a major constraint to sustainable walnut production (Habibi et al., 2025). This situation has substantially intensified the urgency of identifying drought-tolerant walnut genotypes for use in breeding programs aimed at developing resilient rootstocks and cultivars adapted to water-limited environments. The challenge is particularly critical during the seedling stage, where DS can exert disproportionate and irreversible effects on walnut growth, establishment, and long-term vigor, ultimately restricting orchard productivity and tree longevity (Guiqing et al., 2024). Despite the economic and ecological importance of walnut, systematic screening and integration of drought tolerance traits, especially at early developmental stages, remain limited, highlighting a clear knowledge gap that hampers progress toward climate-resilient walnut cultivation (Vahdati et al., 2009; Habibi et al., 2024). The diversity observed in native Iranian walnut populations, which grow across a wide range of habitats from extremely arid and rainy to cold and warm conditions, attests that in Iran's natural environment, walnut has evolved a set of morphological, physiological, and molecular adaptations to tolerate abiotic stresses, especially drought. Therefore, understanding the underlying mechanisms of walnut adaptation to environmental conditions is crucial for the conservation of Iran's walnut genetic resources under the challenges posed by climate change.

Genetic diversity is one of the most critical factors for success in plant breeding programs. Such diversity collections enable more accurate evaluation of germplasm and identification of promising genotypes for breeding purposes. The major challenges faced by walnut breeding programs is managing a large number of genotypes while maintaining genetic diversity and simultaneously reducing evaluation and maintenance costs. Furthermore, the evaluation and selection of superior walnut genotypes is highly challenging due to the high genetic variability and the complexity of mechanisms involved in DS response. Moreover, the development of robust methods to identify phenotypic traits associated with drought tolerance is crucial for the advancement of walnut breeding programs. The receiver operating characteristic (ROC) curve provides a powerful statistical approach for evaluating the accuracy and discriminative capability of physiological parameters under DS by analyzing under the curve (AUC) and Youden's Index (YI) metrics to identify key traits and determine optimal thresholds (OT). Although the ROC curve algorithm has been employed in crops like winter wheat (Mu et al., 2021; Ru et al., 2023), its application in tree crops remains limited.

The analysis of large genotype sets, coupled with the multidimensional responses of each genotype across stress-related traits, cannot be sufficiently addressed using conventional statistical methods alone. Therefore, group multi-criteria design making (GMCDM) approaches can be effective for the scientific and systematic selection of superior genotypes (Dragincic et al., 2015; de-Matos Lessa et al., 2024; Wei et al., 2025). Overall, although studies based on GMCDM methods exist in many fields, their application in agriculture, especially for the evaluation of fruit tree cultivars and rootstocks in response to environmental stresses is very limited.

The GMCDM methods, such as hierarchical analysis and ranking techniques, enable accurate weighting of various criteria and comparison of genotypes (Dragincic et al., 2015). These methods, by balancing quantitative and qualitative criteria, have facilitated the identification of genotypes that are not only superior in terms of yield and kernel quality but also possess high potential for use in breeding programs and commercial production (de-Matos Lessa et al., 2024). The application of this approach, by reducing the complexity of multidimensional data analysis, allowed for the selection of optimal genotypes while maintaining genetic diversity (Wei et al., 2025). However, the combined use of these methods can yield varying results depending on the techniques applied, which may cause uncertainty for breeders and researchers in precisely selecting superior genotypes. To address this limitation and enhance the reliability of genotype selection, consensus-based ranking approaches have gained increasing attention. Among these, the Copeland method offers a powerful framework for integrating rankings derived from multiple MCDM techniques by aggregating pairwise

comparisons into a single, coherent score. By synthesizing the outcomes of different decision-making models, the Copeland approach minimizes method-specific bias and reduces ranking instability, thereby providing a more objective and robust prioritization of genotypes (Saari and Merlin, 1996). This integration is particularly valuable in complex biological datasets, where reliance on a single MCDM method may lead to inconsistent or ambiguous conclusions (Heidarzadeh et al., 2020). Consequently, the Copeland-based consensus ranking represents a reliable strategy for identifying superior genotypes with greater confidence for breeding and applied selection programs.

As breeding objectives become increasingly complex, encompassing multiple physiological, biochemical, and agronomic traits, the challenge of accurately identifying superior genotypes has grown substantially. Conventional selection approaches often struggle to synthesize multi-dimensional information from diverse traits, leading to potential biases, inconsistent prioritization, and suboptimal selection decisions. This limitation is particularly critical under environmental stresses such as drought, where the interaction among traits can profoundly influence plant performance and resilience. To overcome these challenges, advanced decision-making frameworks that can systematically integrate multiple criteria and provide a robust, objective basis for genotype selection are essential. In this context, the integration of trait weighting via ROC curve analysis, the application of multiple well-established MCDM techniques, and the use of the Copeland rank aggregation method represent a powerful and reliable strategy to generate a consensus-based ranking. Despite the recognized potential of these approaches, their combined application in evaluating drought tolerance in walnut genotypes remains largely unexplored, revealing a critical knowledge gap in precision breeding under water-limited conditions. Therefore, this study aims to comprehensively assess 183 diverse walnut genotypes across varying climatic conditions in Iran, elucidate the physiological and biochemical mechanisms underlying DS response, and identify superior drought-tolerant genotypes using this integrated, state-of-the-art framework.

2. Materials and methods

2.1. Plant materials and treatments

This study was conducted over three consecutive years. In the first year, seven major walnut-producing provinces of Iran, each characterized by distinct climatic conditions, were selected and based on a questionnaire design and phenotypic evaluation, a total of 183 genotypes were sampled from mountainous areas and long-established walnut orchards. Maternal genotypes, aged between 50 and 350 years, with trunk diameters greater than 50 cm. Due to high heterozygosity and to address the selection of the drought-tolerant genotype, the seeds used in this study were single-seeded (i.e., without replication), and each seed was derived from an individual open-pollinated walnut genotype.

Then, following the protocol established by Vahdati et al. (2009), the seeds were initially soaked in running water for 10 days, disinfected with a 5% Captan fungicide solution, and then stratified at 4–7°C for 720 h. After stratification, seeds were sown in 7-L polyethylene pots (15 × 40 cm) filled with a mixture of soil, sand, and leaf mold (2:1:1). In the second year, the plants were adequately irrigated and fertilized, and at the end of the growing season, uniform and healthy seedlings were selected for planting. In the third year, after completing their chilling requirement and before bud break, genotypes were transplanted into 15-L polyethylene pots (20 × 50 cm) to facilitate better root development.

Plants were cultivated under controlled greenhouse conditions at 25 ±2°C, with a 16-hour light regime and relative humidity maintained between 35% and 50%. Irrigation was applied regularly to preserve consistent soil moisture, and fertilization was conducted monthly using macro- and micronutrient formulations. At 15 months of age, genotypes were established in a common field to assess drought tolerance.

2.2. Applying drought stress

Drought stress (DS) was imposed by water withholding for a period of 30 days. To assess the impact of DS on locally adapted walnut genotypes, the genotypes were randomly assigned to two groups: well-watered group (WW), which received regular irrigation to maintain soil moisture above 75% of field capacity, and Drought stress group (DS), in which irrigation was withheld to reduce soil moisture to approximately 28% of FC (Fig. S1).

2.3. Data collection

2.3.1. Phenotyping of scoring data

A structured scoring method was employed to assess genotype health and appearance under DS. Evaluations were conducted by five DS specialists, who rated each genotype according to three indices: drought tolerance (Scale 1–9), wilting (Scale 1–5), and leaf shedding (Scale 1–5).

2.3.2. Relative water content and membrane stability index

Relative Water Content (RWC) was measured using fresh leaf samples from each plant. RWC was calculated as: RWC (%) = (FW − DW) / (TW − DW) × 100, where FW is fresh weight, TW is turgid weight after 24 h rehydration at 4 °C in the dark, and DW is dry weight after drying at 75 °C for 72 h. The membrane stability index (MSI) was determined by assessing electrolyte leakage. Twenty leaf discs from fully expanded young leaves were used for this measurement.

2.3.3. Photosynthetic pigments and OJIP-test

The chlorophyll *a, b*, total chlorophyll, and carotenoids were evaluated based on the protocol described by Lichtenthaler (1987). Polyphasic chlorophyll fluorescence transients (OJIP-test) were recorded from the same young leaves across all genotypes under both control and drought conditions using a portable fluorometer (Fluorpen FP 100-MAX, Photon Systems Instruments, Drasov, Czech Republic). Before measurement, leaves were dark-adapted for 20 min as described by Aliniaeifard et al. (2014). Definitions and calculation methods for all parameters are presented in Table S1.

2.3.4. H_2O_2 and malondialdehyde content

Hydrogen peroxide (H_2O_2) levels in leaf tissues were quantified using a modified colorimetric assay based on the method of Loreto and Velikova (2001). Fresh leaf samples (0.25 g) were ground in 0.1% trichloroacetic acid, centrifuged, and the supernatant was reacted with phosphate buffer and potassium iodide. Following a one-hour dark incubation, absorbance was recorded at 390 nm. Malondialdehyde (MDA) levels were measured following the method of Heath and Packer (1968), with slight modifications. Fresh leaf tissue (0.25 g) was homogenized in 0.1% TCA, centrifuged, and the supernatant was mixed with 0.5% thiobarbituric acid in TCA. After heating at 95 °C for 15 min, absorbance was recorded at 450, 532, and 600 nm. MDA content was calculated using the formula: MDA = ($A_{532} - A_{600}$) / 155 × 1000.

2.3.5. Osmoregulators

Total soluble carbohydrates were quantified by reacting 0.1 mL of ethanol extract with an Antron reagent, followed by incubation at 90 °C for 10 min. After cooling, absorbance was measured at 625 nm. A standard glucose curve (0–100 mg/g FW) was used for concentration estimation (Dubois et al., 1956). Free proline content was measured by extracting leaf tissues with ethanol, centrifuging the homogenate, and reacting the supernatant with ninhydrin reagent. After heating and cooling, absorbance was recorded at 520 nm, and proline levels were quantified using a standard curve and expressed as μg/g fresh weight (Bates et al., 1973). Glycine betaine content was measured using a colorimetric method (Grieve and Grattan, 1983), where fresh leaf tissue was extracted with distilled water and sulfuric acid, reacted with potassium iodide, and absorbance was read at 365 nm. Concentrations

were calculated from a standard curve and expressed as μg/g fresh weight.

2.3.6. Superoxide dismutase and catalase activity

Superoxide dismutase (SOD) activity was measured in frozen leaf samples (0.5 *g*) ground in liquid nitrogen and extracted with a phosphate buffer (pH 7.5). Following Fridovich's (1986) method, SOD activity was determined based on its ability to inhibit nitro blue tetrazolium (NBT) reduction under light exposure. Absorbance was recorded at 560 nm, and one unit of SOD was defined as the amount of enzyme needed to inhibit 50% of NBT reduction. Results were expressed per mg protein. Catalase (CAT) activity was assessed by tracking the decrease in H_2O_2 absorbance at 240 nm, following a modified method of Cakmak and Marschner (1992).

2.3.7. Drought stress index

To assess distance plasticity between the two treatments for each replicate, the drought stress index (DSI) was computed using the following equation.

$$\mathrm{DSI} = \frac{Drought - Control}{Control} \times 100$$

2.4. Selecting the best walnut genotypes

2.4.1. Step 1: the receiver operating characteristic curve

The initial phase of the genotype selection framework involves ranking the relevant traits based on their ability to discriminate between desirable and undesirable outcomes. This step utilizes two established metrics from the field of binary classification: the Area Under the Receiver Operating Characteristic (ROC) Curve (AUC) and Youden's Index (YI). AUC and YI were selected for their non-parametric nature and independence from trait distribution assumptions, critical for agricultural traits with skewed data (Huang and Ling, 2005). The AUC serves as a measure of a trait's overall ability to distinguish between two classes, representing the probability that a randomly chosen positive instance will be ranked higher than a randomly chosen negative instance. The ROC Curve is a comprehensive measure that reflects the overall ability of a logistic regression model to distinguish between sensitive and resistant outcomes across all classification thresholds by the results of data scoring and clustering of HDBSCAN. This metric is particularly valuable as it considers all possible classification thresholds, providing a comprehensive assessment of the trait's discriminative power. Hanley and McNeil (1982) have extensively discussed the meaning and use of AUC in evaluating diagnostic tests, a concept directly applicable to assessing the discriminatory power of traits in genotype selection. Furthermore, recent research by Li (2024) has highlighted the consistency of AUC in evaluating and ranking models across various scenarios, underscoring its reliability. The ranking of traits based on AUC is performed in descending order, with traits exhibiting higher AUC values receiving a better rank. This can be mathematically represented as:

$$R_{AUC}(i) = Rank(AUC(i)) \tag{1}$$

where i denotes a specific trait, $AUC(i)$ is the AUC value calculated for that trait, and $R_{AUC}(i)$ represents the rank of the trait i based on its AUC value, with a lower rank number indicating a higher AUC.

In conjunction with AUC, Youden's Index (YI) is employed to evaluate the effectiveness of each trait in balancing sensitivity and specificity. YI is calculated as the sum of sensitivity and specificity minus one (Sensitivity + Specificity - 1) and represents the maximum vertical distance between the ROC curve and the line of no discrimination. This index provides a measure of the trait's ability to correctly identify positive cases while minimizing false positives. The original formulation of Youden's Index was introduced by Youden in 1950, and subsequent studies, such as those by Fluss et al. (2005) and Shan (2015), have further explored its properties and applications in diagnostic testing and biomarker evaluation. Similar to AUC, traits are ranked based on their YI values in descending order, with higher YI values indicating better performance and thus receiving a better rank. The equation for this ranking is:

$$R_{YI}(i) = Rank(YI(i)) \tag{2}$$

where i represents a specific trait, $YI(i)$ is the Youden's Index value for that trait, and $R_{YI}(i)$ is the rank of the trait i based on its YI value, with a lower rank signifying a higher YI.

2.4.2. Step 2: normalized weight calculation

To derive a comprehensive weight that reflects the importance of each trait, the ranks obtained from both AUC and YI are aggregated. This is achieved by first calculating the average rank for each trait:

$$\overline{R}(i) = \frac{R_{AUC}(i) + R_{YI}(i)}{2} \tag{3}$$

where i represents a specific trait, $R_{AUC}(i)$ is its rank based on AUC, and $R_{YI}(i)$ is its rank based on YI. This averaging step provides a balanced assessment of the trait's performance across two complementary metrics. Following the calculation of the average rank, a normalized weight for each trait is determined. This weight is inversely proportional to the average rank, ensuring that traits with better average ranks (lower values) receive higher weights, thus reflecting their greater importance in the selection process. The normalized weight is calculated using the following formula:

$$W(i) = \frac{11\overline{R}(i)\overline{R}(i)}{\sum_{j=1}^{n} 1 \Big/ (\overline{R}(j))} \tag{4}$$

where i is the trait for which the weight is being calculated, $\overline{R}(i)$ is its average rank, and the summation in the denominator is performed over all relevant traits j. This normalization ensures that the weights assigned to all traits sum to 1, providing a standardized measure of their relative importance that can be used in subsequent multi-criteria decision-making methods.

2.4.3. Step 3: apply the MCDM models: MCDM methods

To obtain a robust and multifaceted ranking of genotypes, this framework employs a suite of prominent Multi-Criteria Decision-Making (MCDM) methods. Each method utilizes the normalized weights and the performance data of each genotype across the selected traits to generate a ranked list of genotypes. The application of multiple MCDM methods, which are based on different aggregation principles, allows for a more comprehensive evaluation of the genotypes, mitigating potential biases inherent in a single method. The following MCDM methods are applied:

- **ELECTRE** (Elimination and Choice Translating Reality): This outranking method compares pairs of genotypes based on the concepts of concordance and discordance. It assesses the strength of the hypothesis that one genotype outranks another by considering the weighted sum of criteria where the first genotype performs at least as well as the second (concordance) and by evaluating whether any criterion shows a sufficiently large difference in performance to refute this hypothesis (discordance). Preference and indifference thresholds are used to define these relationships more precisely. The foundations of ELECTRE were laid by Roy (1991), and comprehensive overviews are provided by Figueira et al. (2013).
- **SAW** (Simple Additive Weighting): This method calculates a total score for each genotype by taking a weighted sum of its performance across all traits. The performance of each genotype on each trait is multiplied by the normalized weight of that trait, and these products are summed to yield the overall score. Genotypes are then ranked based on these scores, with higher scores indicating better overall

performance. Hwang and Yoon (1981) provide a foundational text on MCDM methods, including SAW, and recent guides by Taherdoost (2023) offer detailed explanations of its application.

- **TOPSIS** (Technique for Order of Preference by Similarity to Ideal Solution): This method ranks genotypes based on their proximity to an ideal solution (representing the best performance on all traits) and their distance from a negative-ideal solution (representing the worst performance on all traits). The preferred genotype is the one that is closest to the ideal and farthest from the negative-ideal. TOPSIS was originally developed by Hwang and Yoon (1981), and a step-by-step guide is available in works like Madanchian and Taherdoost (2023).
- **VIKOR** (VlseKriterijumska Optimizacija I Kompromisno Resenje): This compromise ranking method determines a solution that is closest to the ideal by considering the majority of criteria and the minimization of individual regret. It calculates three values for each genotype: the utility measure based on the distance from the ideal solution, the individual regret measure based on the maximum deviation from the best performance on any criterion, and a compromise measure that combines these two. Genotypes are ranked based on these values to identify the one offering the best compromise. The VIKOR method was developed by Opricovic (1998), and its comparative analysis with other MCDM methods is discussed by Opricovic and Tzeng (2004).

Each of these MCDM methods will process the decision matrix, where genotypes are the alternatives and traits are the criteria, using the previously calculated normalized weights for the traits. This will result in four distinct ranked lists of genotypes, each reflecting a different approach to aggregating the multi-criteria information.

2.4.4. Step 4: pairwise comparison of the genotypes

To synthesize the multiple ranked lists of genotypes obtained from the different MCDM methods, the Copeland method, a robust rank aggregation technique based on pairwise comparisons, is employed. This method facilitates a head-to-head evaluation of each genotype against every other genotype based on their relative positions in the rankings produced by ELECTRE, SAW, TOPSIS, and VIKOR. A pairwise comparison matrix is constructed where both the rows and columns represent the genotypes under evaluation. For each pair of genotypes (e.g., Genotype A and Genotype B), their relative ranking across the four MCDM output lists is examined. If Genotype A ranks higher than Genotype B in a particular MCDM ranking, a score of $+1$ is assigned to A in the comparison matrix. If the two genotypes are tied in a given MCDM ranking, no score is awarded (0 points). This ensures that ties do not contribute to the final score, focusing only on instances where one genotype is definitively preferred over another. This process is repeated for all pairs of genotypes across all four MCDM ranking lists, effectively summarizing the number of times each genotype is preferred over every other genotype according to the different MCDM methods.

2.4.5. Step 5: Copeland score calculation

Once the pairwise comparison matrix is constructed, a Copeland Score is calculated for each genotype. This score is determined by summing the number of "wins" (where the genotype ranked higher) and subtracting the number of "losses" (where the genotype ranked lower) in all the pairwise comparisons across the different MCDM rankings. Mathematically, the Copeland Score for a genotype A is given by:

$$Copelan\ Score(A) = \alpha - \beta \tag{5}$$

where α represents the total number of times Genotype A ranked higher than other genotypes across all MCDM methods, and β represents the total number of times Genotype A ranked lower than other genotypes across all MCDM methods. The foundational work on the Copeland method was presented by Copeland in 1951, with further analysis and applications discussed by Saari and Merlin (1996). The Copeland Score provides a single numerical value that reflects the overall preference for a genotype based on the collective evidence from the multiple MCDM analyses. A higher Copeland Score indicates that a genotype was preferred more often in the pairwise comparisons, suggesting a stronger overall ranking.

2.4.6. Step 6: final genotype ranking

The final step in the genotype selection framework involves ranking the genotypes based on their calculated Copeland Scores (Fig. 1). The genotypes are sorted in descending order of their Copeland Scores, with the genotype exhibiting the highest score being considered the top-ranked choice. This final ranking represents a consensus derived from the integration of four different MCDM methods, providing a more robust and reliable selection of superior genotypes.

2.4.7. Path analysis and multicollinearity assessment

To determine the mechanistic hierarchy of traits contributing to the final ranking, a path analysis was performed. This analysis decomposed the total Pearson correlation coefficients between the measured traits and the final Copeland scores into direct P_i and indirect effects. The direct effect represents the unique contribution of a trait to the drought tolerance score, while indirect effects quantify the influence mediated through other interdependent variables. To ensure the reliability of the model and address concerns regarding criterion independence in the MCDM framework, multicollinearity was assessed using the Variance Inflation Factor (VIF). A VIF threshold of <10 was considered acceptable for complex biological systems.

2.4.8. Multivariate divergence using Mahalanobis D^2 statistics

To validate the physiological distinctness of the genotype clusters identified by DBSCAN, Mahalanobis D^2 statistics were employed. The D^2 statistic measures the multivariate distance between the centroids of different groups while accounting for the covariance structure of the data. This analysis served as an independent validation of the "Tolerant" and "Sensitive" groupings, ensuring that the binary classes used for ROC-based weighting represented significant physiological divergence rather than methodological artifacts.

2.4.9. Ranking stability and LOMO cross-validation

The robustness of the final Copeland-based ranking was evaluated using a "Leave-One-Method-Out" (LOMO) cross-validation approach. In this sensitivity analysis, the Copeland scores were iteratively recalculated by sequentially excluding one of the four MCDM methods (TOPSIS, SAW, VIKOR, or ELECTRE). The stability of the ranking was quantified using Spearman's Rank Correlation Coefficient ρ between the full consensus model and each sub-model configuration. High correlation values $\rho > 0.90$ and the stability of top-ranked genotypes across all iterations was used to confirm the reliability of the decision-making framework.

2.5. Statistical analyses

The Shapiro-Wilk test was utilized to assess the normal distribution of each trait. Descriptive statistics, T-test, and frequency distributions were conducted using Prism software. The classification of samples into "resistant" and "susceptible" groups for ROC analysis was determined based on the HDBSCAN clustering results and subsequently validated against the observer scores. For cluster analysis of the genotypes, the DBSCAN algorithm was applied using the *dbscan* package in R. All visualizations were generated using the ggplot2 package. The analyses involving VIF, Mahalanobis D^2 statistics, and path analysis were implemented in Python (version 3.10) using SciPy (version 1.16.3) (Virtanen et al., 2020) and statsmodels (version 0.14.6) (Seabold and Perktold, 2010). Additionally, analyses related to Multi-Criteria Decision Making (MCDM) methods and the Copeland ranking technique were conducted using scikit-learn (version 1.3.0) (Pedregosa et al.,

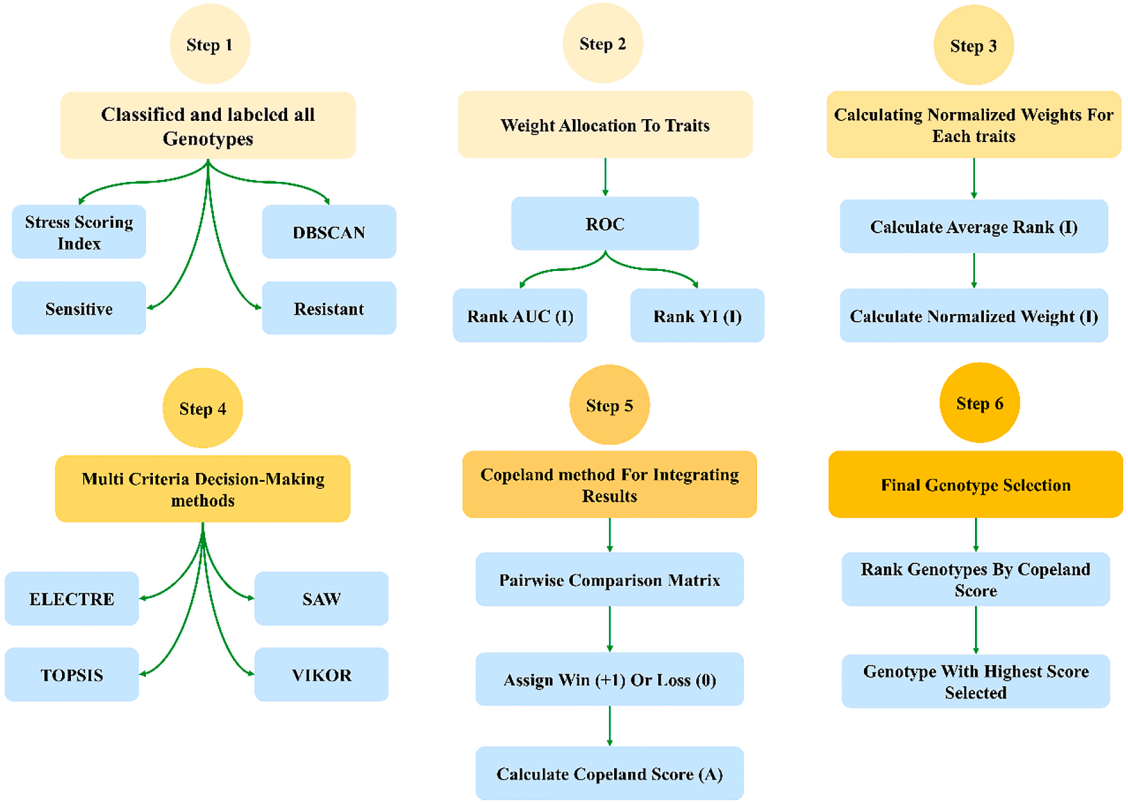

Fig. 1. Schematic of how to rank and select superior drought-tolerant genotypes based on Multi-Criteria Decision Making (MCDM) methods and the Copeland ranking technique.

2011) for pairwise computations, pandas (version 2.0.3) (McKinney, 2010) for data structuring and manipulation, and NumPy (version 1.24.0) (Harris et al., 2020) for efficient numerical operations and algorithmic implementations.

3. Results

3.1. Descriptive statistics

Descriptive statistical results and frequency distributions (Figs. 2, 3, Table S1) included the maximum, minimum, and mean values of different parameters under control and drought stress (DS), the differences between the means, and the percentage changes induced by DS.

The findings revealed that DS had a significant impact on the evaluated parameters. The mean relative water content (RWC) under drought conditions (50.27) showed a sharp decrease compared to the control (79.34), with a difference of 29.08 units, equivalent to a 36.63% reduction. Similarly, the total chlorophyll (TChl) content decreased by 495 units (29.67%) under DS (mean of 1680.34) compared to the control (2175.8). Carotenoid content also declined under drought (mean of 677.64) compared to the control (793.42), showing a reduction of 118.3 units or 17.51%. Among osmolyte regulators, the highest percentage increases were observed in glycine betaine (GB), total soluble sugars (TSS), and proline, with increases of 89.63%, 91.06%, and 45.9%, respectively.

Regarding oxidative markers, the mean membrane stability index (MSI) under DS (49.108) decreased by 29.48 units compared to the control (78.68), representing a 37.58% reduction. In contrast, hydrogen peroxide (H_2O_2) and malondialdehyde (MDA) showed substantial increases of 115% and 266%, respectively. Additionally, antioxidant enzyme activities increased significantly, with 64% and 115% increases observed in superoxide dismutase (SOD) and catalase, respectively.

Furthermore, among chlorophyll fluorescence indices, the greatest reduction was observed in the performance index per absorbed photon (PI_{ABS}) by 68.55%, followed by decreases in the maximum efficiency of the water-splitting complex on the donor side of PSII (F_V/F_0) by 47.61%, the ratio of maximal to minimal chlorophyll fluorescence (F_M/F_0) by 45.46%, and the maximum quantum yield of photosystem II (F_V/F_M) by 36.33%.

3.2. Phenotyping of scoring data

Phenotyping of traits related to walnut genotypes' health under DS conditions revealed that the evaluated genotypes exhibited varying responses, as indicated by the descriptive statistics of the scoring data. As shown in Table 1, under drought conditions, the severity of wilting, leaf drop in walnut genotypes, and the drought sensitivity index increased. For the trait Wilting, values ranged from 1 to 5, with a mean of 3, a standard deviation of 1.38, and the highest coefficient of variation (45.83%), indicating substantial variability among genotypes in terms of wilting severity. Leaf Drop had a minimum and maximum of 1 and 5, respectively, with a mean of 3.47, a standard deviation of 1.43, and a coefficient of variation of 41.18%, reflecting moderate variability among genotypes. Finally, the drought score index (DSI) ranged from 1 to 9, with a mean value of 4.80, a standard deviation of 2.17, and a coefficient of variation of 45.17%, suggesting considerable diversity among genotypes for this trait.

3.3. Clustering analysis

In this study, a clustering analysis using the DBSCAN method were performed to differentiate 183 diverse Persian walnut genotypes after 30 days of DS, based on physiological, photosynthetic, and biochemical traits (Fig. 4). According to the clustering analysis results, the genotypes were grouped into three clusters: Cluster 0 (11 genotype), Cluster 1 (31 genotype) and Cluster 2 (141 genotypes) (Fig. 4).

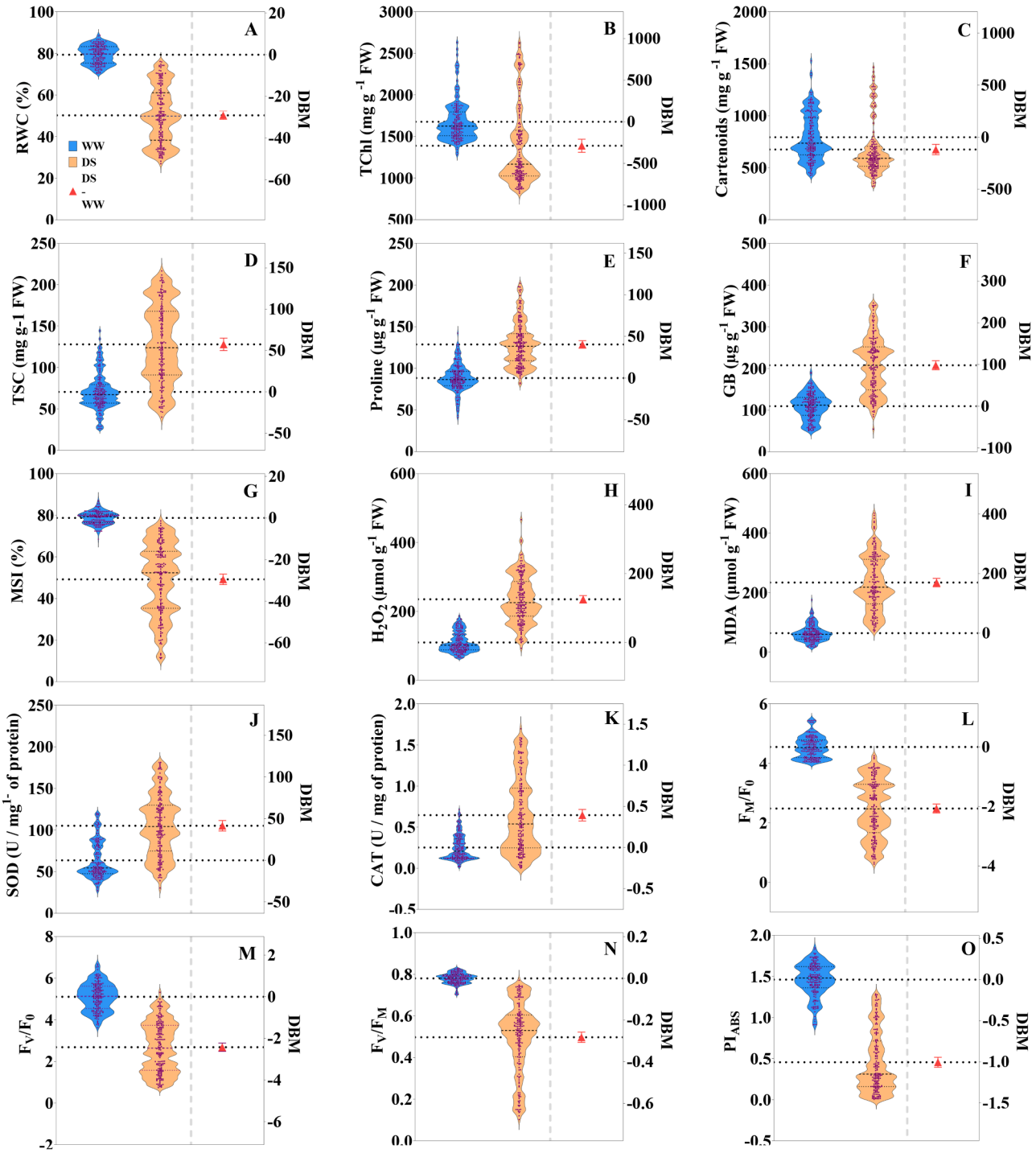

Fig. 2. Violin plot illustrating the differentiation of (A) relative water content (RWC), (B) total chlorophyll (TChl), (C) carotenoids, (D) total soluble carbohydrate (TSC), (E) proline, (F) glycine betaine (GB), (G) membrane stability index (MSI), (H) hydrogen peroxide (H_2O_2), (I) malondialdehyde (MDA), (J) superoxide dismutase (SOD), (K) catalase (CAT), (L) the maximal and minimum chlorophyll fluorescence (F_M/F_0), (M) the Maximum efficiency of the water diffusion reaction (F_V/F_0), (N) the maximum quantum yield of photosystem II (PSII) (F_V/F_M), (O) performance index per absorbed photon (PI_{ABS}) in Persian walnut genotypes difference under well water (WW) and Drought stress (DS). DBM: difference between means. The differences between the control and drought stress conditions for all traits were statistically significant at $p < 0.01$ (T-test).

Subsequently, to rank the genotypes under DS, an initial framework was established based on the measured traits' ability to differentiate between favorable and unfavorable outcomes among the genotypes under DS. The results of the trait ranking are presented in Table 2, based on the Area under the Receiver Operating Characteristic Curve (AUC) and Youden's Index (YI). The AUC and YI values, along with precise weighting for each trait, are reported. The traits were ranked in descending order based on their AUC and YI values, with traits exhibiting higher AUC and YI values receiving better ranks. According to the results of the feature selection method and the evaluation of feature stability across the studied genotypes, traits such as F_M/F_0, MSI, F_V/F_M, PI_{ABS}, MDA, and RWC achieved the highest scores, while traits such as Chl b, SOD, catalase, and carotenoids had the lowest weights. The weighting results for all traits are presented in Table 2.

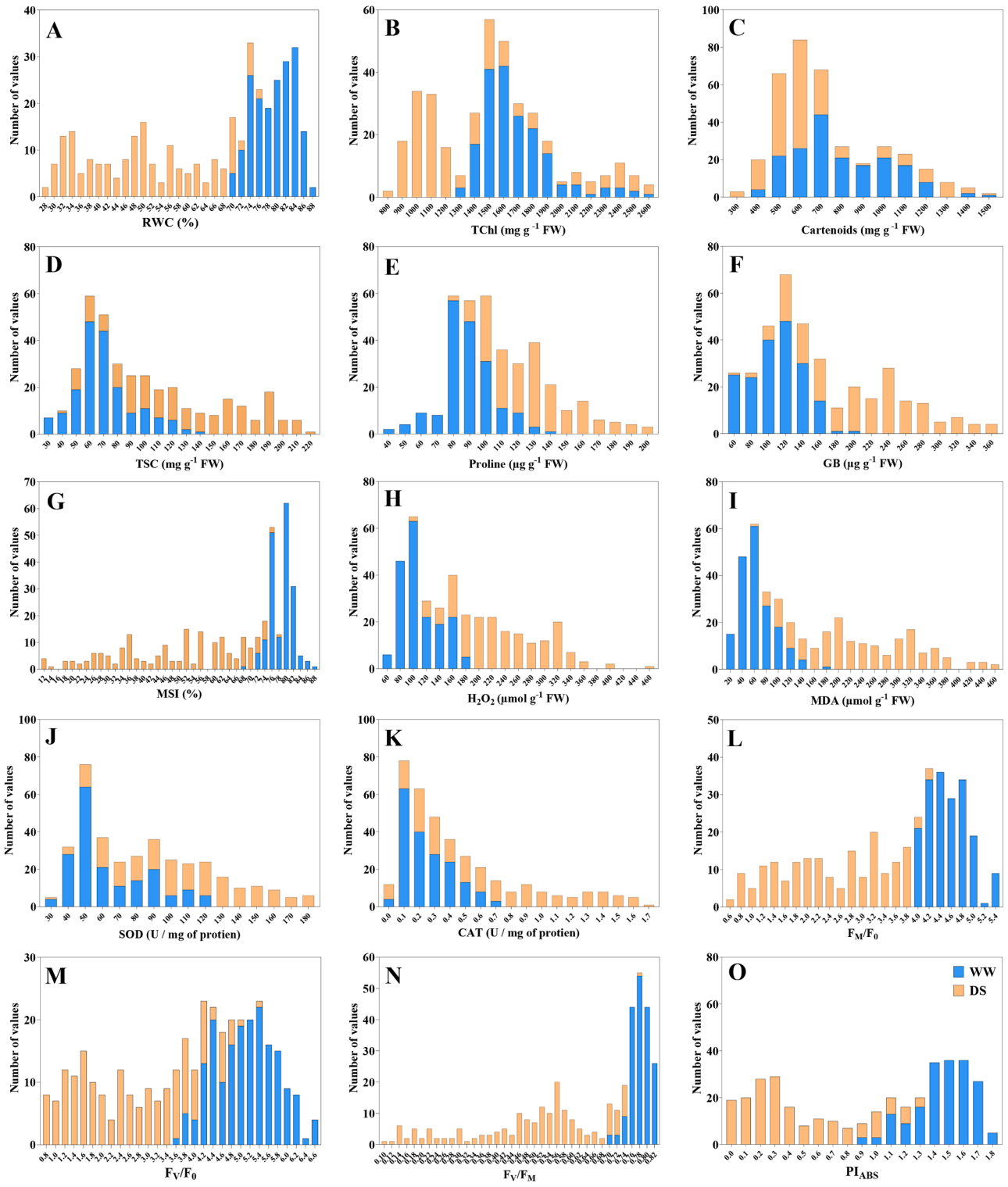

Fig. 3. Frequency distributions plot for various physiological, biochemical and photosynthesis traits of Persian walnut difference genotypes under well water (WW) and drought stress (DS): (A) relative water content (RWC), (B) total chlorophyll (TChl), (C) carotenoids, (D) total soluble carbohydrate (TSC), (E) proline, (F) glycine betaine (GB), (G) membrane stability index (MSI), (H) hydrogen peroxide (H_2O_2), (I) malondialdehyde (MDA), (J) superoxide dismutase (SOD), (K) catalase (CAT), (L) the maximal and minimum chlorophyll fluorescence (F_M/F_0), (M) the Maximum efficiency of the water diffusion reaction (F_V/F_0), (N) the maximum quantum yield of photosystem II (PSII) (F_V/F_M), (O) performance index per absorbed photon (PI_{ABS}).

3.4.1. The ROC curve analysis

The ROC curve analysis identified the most critical indices for evaluating vulnerabilities under DS. This approach effectively measures the accuracy and discriminative power of various traits to identify stress conditions. Based on the area under the curve (AUC) and Youden's Index (YI) from this experiment, certain traits demonstrated superior performance in distinguishing plants under DS (Table 1, Fig. 5).

For photosynthetic performance traits derived from the OJIP test, due to its high AUC and favorable YI, F_V/F_M was recognized as a valuable tool for screening drought-resistant genotypes. Following, PI_{ABS}

Table 1
Descriptive statistics of Phenotyping of Scoring Data for 183 native Persian walnut genotypes.

Variable	Min	Max	Mean	Std. Deviation	Std. Error	CV (%)
Drought Score Index	1	9	4.803	2.17	0.1604	45.17
Leaf Drop	1	5	3.47	1.429	0.1056	41.18
Wilting	1	5	3	1.375	0.1016	45.83

was the top-performing index with an AUC of 0.9961 and YI of 0.9556, displaying its high discriminative ability. Other indices, including F_V/F_0 (AUC: 0.9464, YI: 0.7955) and F_M/F_0 (AUC: 0.897, YI: 0.7209), also demonstrated good predictive performance for identifying selection of genotypes (Table 1, Fig. 5).

Among physiological traits, TChl (AUC: 0.9915, YI: 0.9158), Carotenoids (AUC: 0.9892, YI: 0.9139) and RWC (AUC: 0.9739, YI: 0.9026) emerged as the most robust indicator with a making it highly effective for identifying superior genotypes (Table 1, Fig. 2A). Regarding oxidative markers and antioxidant enzymes, MSI demonstrated the highest diagnostic accuracy, with an AUC of 0.9685 and YI of 0.858, outperforming other traits such as SOD (AUC: 0.9516, YI: 0.805), H_2O_2 (AUC: 0.9339, YI: 0.8099), CAT (AUC: 0.9141, YI: 0.7293), and MDA (AUC: 0.894, YI: 0.7132) (Table 1, Fig. 5). In terms of osmotic regulators, the predictive power was comparatively lower. Glycine betaine (AUC: 0.9368, YI: 0.8231) performed better than proline (AUC: 0.8907, YI: 0.7132) and TSC (AUC: 0.8872, YI: 0.6716) (Table 1, Fig. 5). Despite their relatively lower AUC and YI values, these traits still provided meaningful insights into plant responses under DS.

3.4.2. Optimal threshold

The results regarding the optimal threshold (OT) for physiological traits highlight varying performances of different indices in predicting DS in Persian walnut difference genotypes (Table 1). The OT values for photosynthetic performance traits were as follows: F_M/F_0 (3.206), F_V/F_0 (3.802), F_V/F_M (0.6365), PI_{ABS} (0.89). Additional indices and their

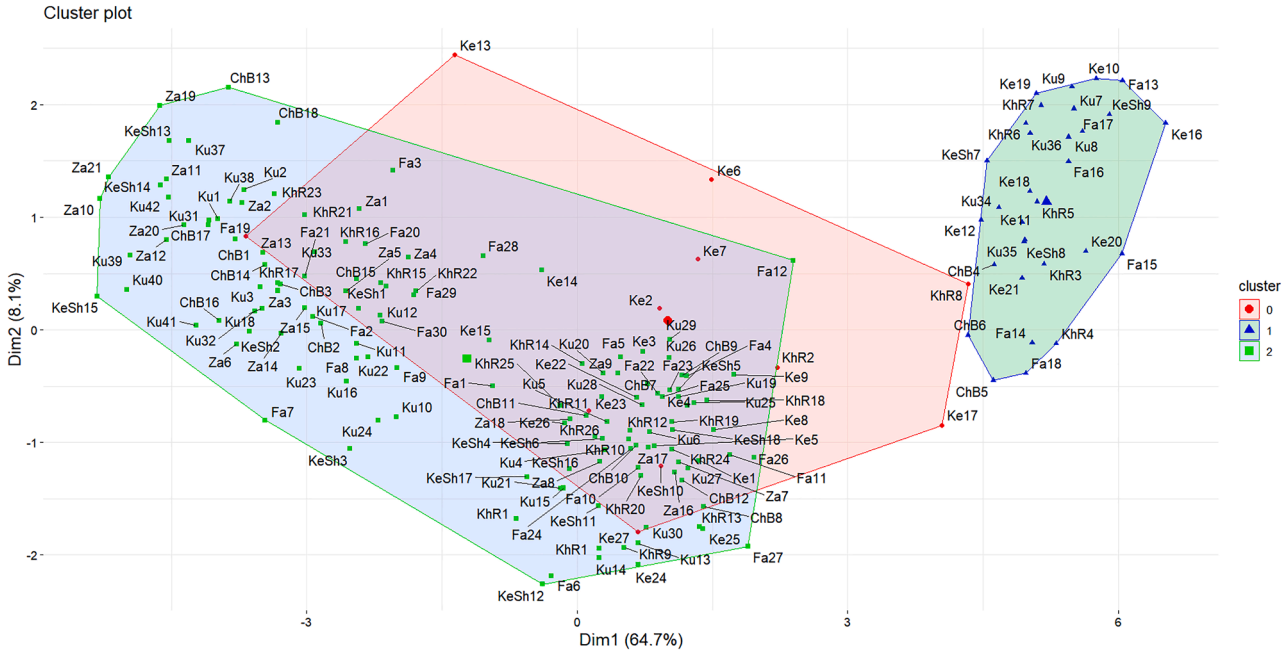

Fig. 4. Cluster analysis based on the DBSCAN method related to physiological, photosynthetic, and biochemical traits in 183 Persian walnut genotypes under drought stress conditions after 30 days.

Table 2
Summary of variable importance based on Best optimal, Area Under the Curve (AUC), and Youden's Index (YI), including their corresponding scores (AUC Score and YI Score), average ranks, and assigned weights. The Direction column indicates whether a higher or lower value is desirable for each variable. See Fig. 2 for the definition of measured traits.

Variable	Best Optimal	Direction	AUC	YI	AUC Score	YI Score	Average Rank	Weight
F_V/F_M	0.6365	Max	0.9965	0.9669	1	1	1.0	0.301775
PI_{ABS}	0.89	Max	0.9961	0.9556	2	2	2.0	0.150888
TChl	2526	Max	0.9915	0.9158	3	3	3.0	0.100592
Carotenoids	708.0	Max	0.9892	0.9139	4	4	4.0	0.07544
RWC	62.70	Max	0.9739	0.9026	5	5	5.0	0.060355
MSI	64.01	Max	0.9685	0.8580	6	6	6.0	0.050296
SOD	127.0	Max	0.9516	0.8050	7	8	7.5	0.040237
H_2O_2	195.6	Min	0.9339	0.8099	10	7	8.5	0.035503
F_V/F_0	3.802	Max	0.9464	0.7955	8	9	8.5	0.035503
GB	244.5	Max	0.9368	0.7198	9	12	10.5	0.028741
CAT	0.9393	Max	0.9141	0.7293	11	10	10.5	0.028741
F_M/F_0	3.206	Max	0.8970	0.7209	12	11	11.5	0.026241
Proline	146.9	Max	0.8907	0.7198	14	12	13.0	0.023213
MDA	156.7	Min	0.8940	0.7132	13	14	13.5	0.022354
TSC	162.2	Max	0.8872	0.6716	15	15	15.0	0.020118

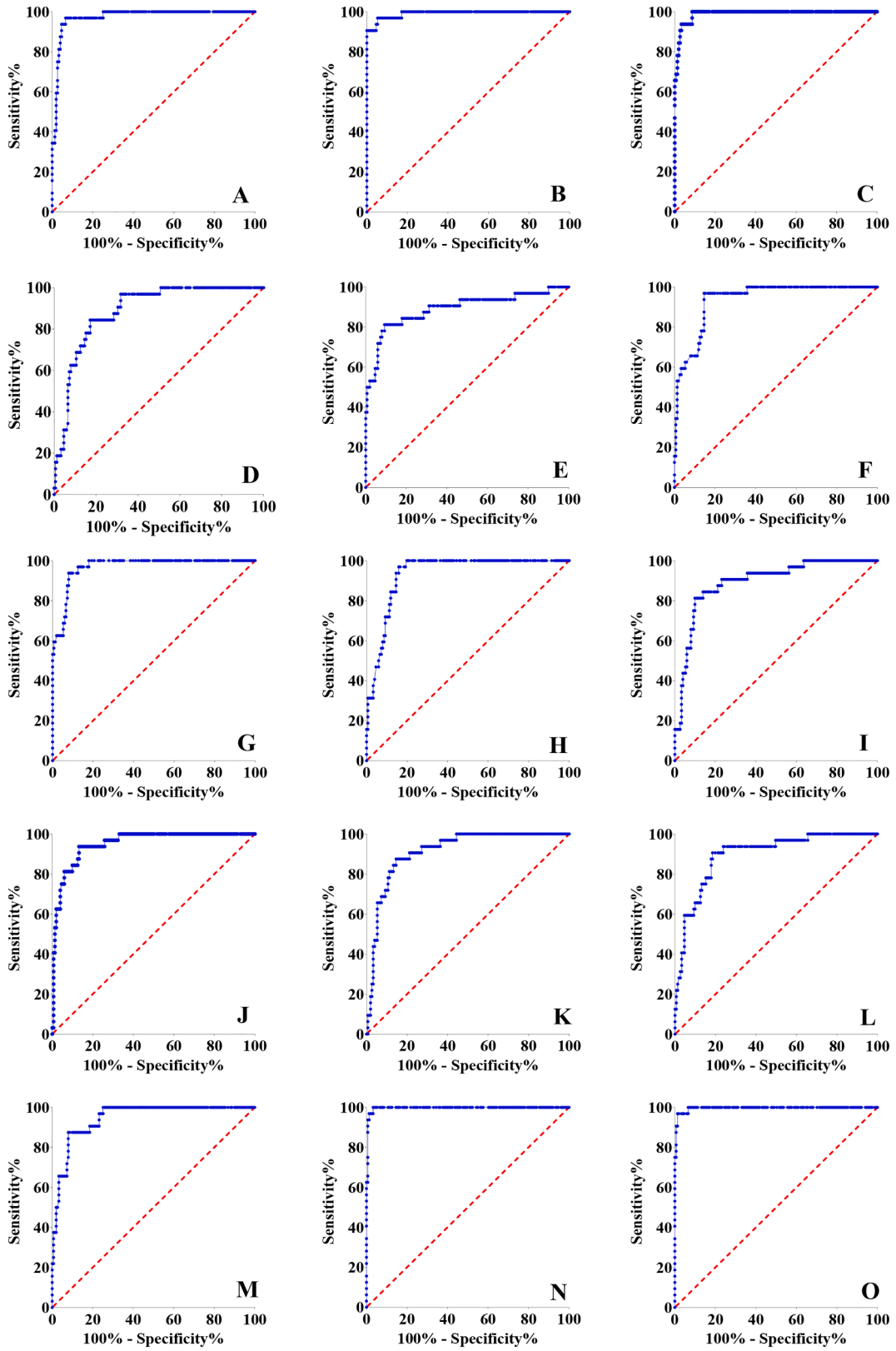

Fig. 5. Receiver Operating Characteristic (ROC) curve analysis for various physiological, biochemical and photosynthesis traits of Persian walnut genotypes under Drought stress: (A) relative water content (RWC), (B) total chlorophyll (TChl), (C) carotenoids, (D) total soluble carbohydrate (TSC), (E) proline, (F) glycine betaine (GB), (G) membrane stability index (MSI), (H) hydrogen peroxide (H_2O_2), (I) malondialdehyde (MDA), (J) superoxide dismutase (SOD), (K) catalase (CAT), (L) the maximal and minimum chlorophyll fluorescence (F_M/F_0), (M) the Maximum efficiency of the water diffusion reaction (F_V/F_0), (N) the maximum quantum yield of photosystem II (PSII) (F_V/F_M), (O) performance index per absorbed photon (PI_{ABS}).

corresponding OT included TChl (2526), carotenoids (708), and RWC (62.7), demonstrating their diagnostic significance. The RWC index exhibited an OT of 70.52%, indicating its effectiveness in identifying DS. Additional indices and their corresponding OT included SPAD (32.09), Chl *a* (1927), Chl *b* (682.8), TChl (2541), and carotenoids (659.9), demonstrating their diagnostic significance. For osmotic regulators, the determined OT were proline (146.9), GB (244.5), and TSC (162.2). In the category of oxidative markers and antioxidant enzymes, the OT identified were 64.01 for MSI, 195.6 for H_2O_2, and 156.7 for MDA. Among enzymes, CAT had an OT of 0.9393, while SOD had an OT of 127 (Table 1).

3.5. Result of group multi-criteria decision-making methods

Fig. 6 presents the ranking outcomes of 183 diverse genotypes from multiple provinces, evaluated under DS using Group Multi-Criteria Decision-Making (GMCDM) methods. In the analysis conducted with the VIKOR method, the genotypes Ke16, KeSh9, Ke20, Ke18, Fa15, Fa16, KhR5, Ku8, KeSh8, and Ke21 were identified as the top 10 genotypes (Fig. 6-A). In the TOPSIS method, the genotypes Ke16, KeSh9, Ke18, KhR5, Fa16, Fa15, Ku8, KeSh8, and KhR4 ranked among the top positions (Fig. 6-B). Additionally, based on the SAW method, the genotypes KeSh9, Ke16, Ke18, Fa16, Fa15, KhR5, Ku8, KeSh8, KhR4, and Fa17 were sequentially recognized as the top 10 options (Fig. 6-C). According to the ELECTRE Score method, the genotypes Ke16, KeSh9, KhR5, Fa15, Ke20, Fa16, Ke18, KeSh8, Ku8, and KhR4 were ranked from 1 to 10, respectively (Fig. 6-D). Detailed and comprehensive ranking results for the 183 genotypes are reported in Supplementary Table 1. Overall, the ranking results of the genotypes varied depending on the GMCDM method employed. For instance, the genotype Ke16 secured the top rank in three methods, ELECTRE, VIKOR, and TOPSIS, while the genotype KeSh9 ranked first in the SAW method. Furthermore, the rankings from second place onward also differed across the methods, highlighting the influence of the decision-making method on the final ranking order of the genotypes. These variations could play a significant role in the final selection of superior genotypes for breeding or research programs.

3.6. Result of the Copeland aggregation method

To achieve consistency in ranking and to obtain a more comprehensive evaluation of the studied genotypes' performance under DS conditions, the Copeland aggregation method was employed. In this method, the scores obtained by each genotype across the four multi-criteria decision-making methods SAW, TOPSIS, VIKOR, and ELECTRE Score were combined and analyzed (Fig. 7). The results of the Copeland classification indicated that the genotypes Ke16, KeSh9, Ke18, Fa15, Fa16, KhR5, Ke20, Ku8, KeSh8, and KhR4 ranked from 1 to 10, respectively. These genotypes, achieving the highest cumulative scores, were identified as the most drought-tolerant. Conversely, genotypes with lower scores in this method were considered more susceptible to DS. Detailed and comprehensive ranking results for the 183 genotypes are reported in Supplementary Table 1.

3.7. Correlation analysis

In this study, strong positive and negative correlations were observed between all measured traits under DS conditions (Fig. 8). These findings provide valuable insights for identifying promising drought-responsive traits, which can be utilized in breeding programs for fruit trees. Physiological, photosynthetic, and biochemical traits are generally interdependent in plants, and significant correlations among them are anticipated.

There was a notable positive correlation between RWC with MSI (0.75), SOD (0.66), CAT (0.63), TChl (0.66), carotenoids (0.54), GB (0.66), TSC (0.58), and proline (0.51), and a negative correlation with H_2O_2 (-0.74) and MDA (-0.68). Furthermore, we observed a significant

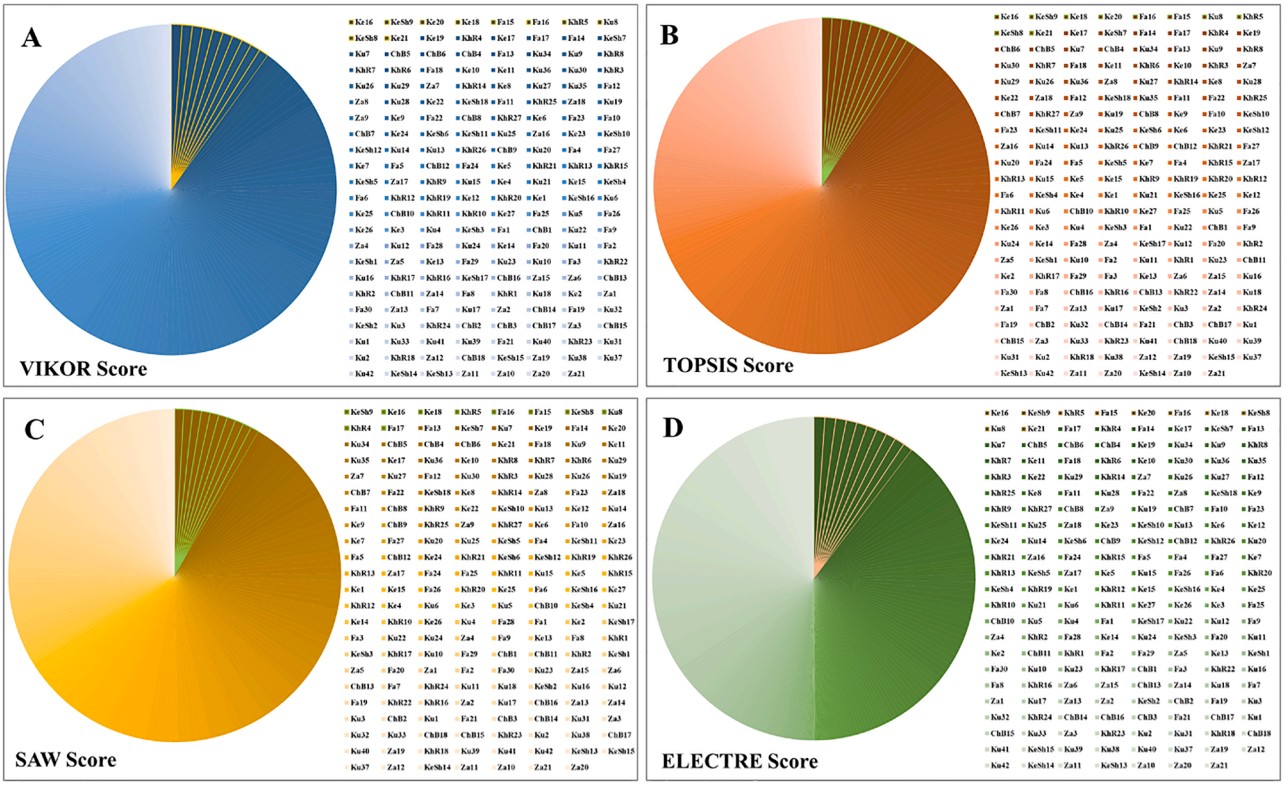

Fig. 6. Results of the ranking of 183 diverse genotypes from various provinces under drought stress conditions using group multi-criteria decision-making (GMCDM) methods, including A) Vikor, B) Topsis, C) SAW, and D) ELECTRE. The ranking order follows a clockwise direction. The top 10 genotypes are highlighted in the chart using distinct colors.

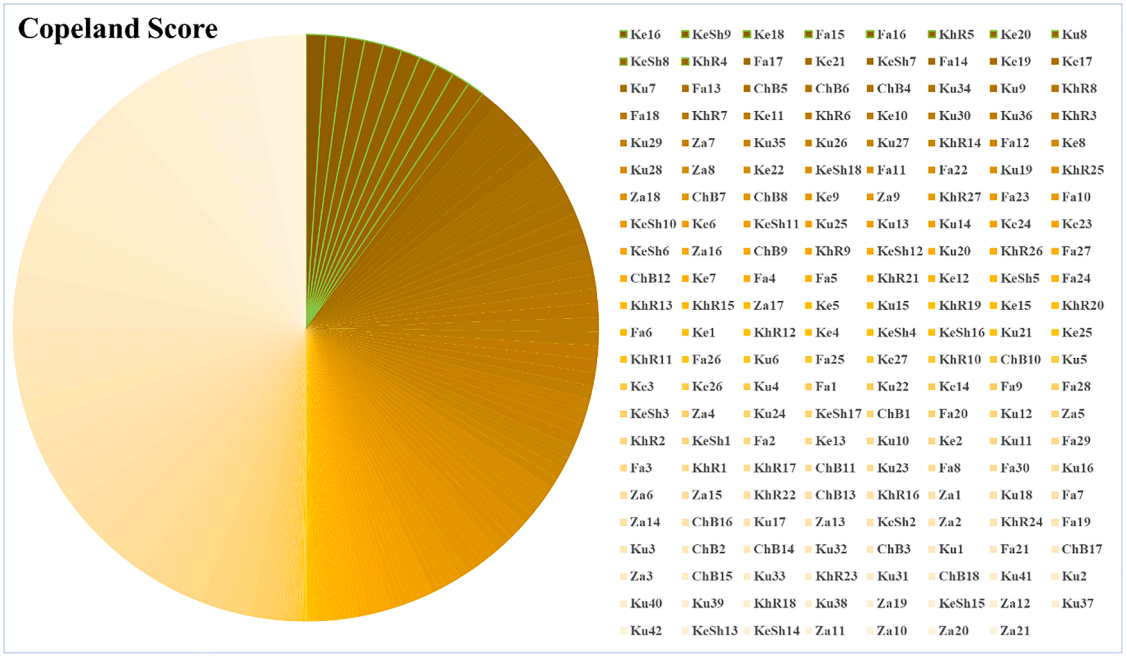

Fig. 7. Results of the ranking of 183 diverse genotypes from various provinces under drought stress conditions using the Copelan method. The ranking order follows a clockwise direction. The top 10 genotypes are highlighted in the chart using distinct colors.

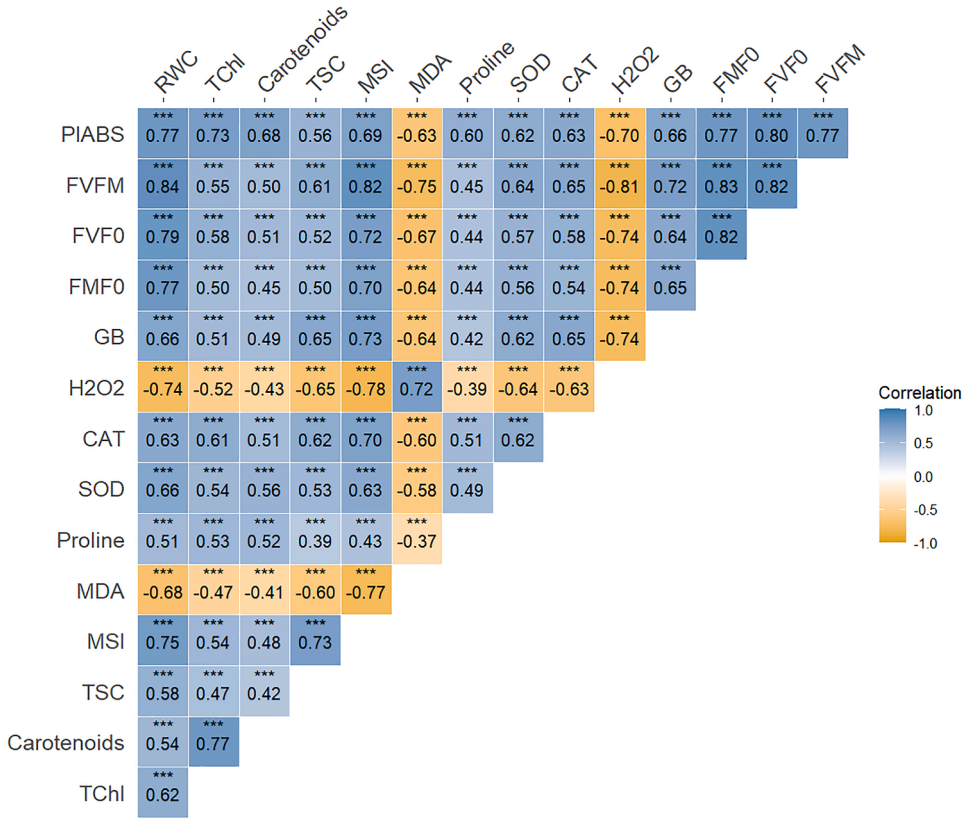

Fig. 8. Correlation coefficients between phenotypic traits of Persian walnut genotypes grown in a common garden under drought stress conditions. The color spectrum, from cadet blue to bright gold, represents highly positive to highly negative correlations. Stars within circles indicate the significance of correlations (*$P \leq$ 0.05, **$P \leq$ 0.01, and ***$P \leq$ 0.001). See Fig. 2 for the definition of measured traits.

positive correlation between RWC and F_V/F_M, F_M/F_0, PI_{ABS}, and F_V/F_0 ($R^2 = 0.84$, $R^2 = 0.77$, $R^2 = 0.77$, and $R^2 = 0.79$, respectively) (Fig. 8). In addition, among photosynthetic traits F_V/F_M had a positive correlation with F_M/F_0 ($R^2 = 0.83$), F_V/F_0 ($R^2 = 0.82$), and PI_{ABS} ($R^2 = 0.77$).

MSI showed significant positive correlation with F_V/F_M ($R^2 = 0.82$), F_M/F_0 ($R^2 = 0.70$), PI_{ABS} ($R^2 = 0.69$), F_V/F_0 ($R^2 = 0.72$), TChl ($R^2 =$

0.54), GB ($R^2 = 0.73$), proline ($R^2 = 0.43$), and SOD ($R^2 = 0.63$). On the other hand, we found a negative and positive correlation between MSI with H_2O_2 and MDA (R^2 = -0.78 and R^2 = -0.77, respectively) (Fig. 8).

3.8. Relationships among physiological indicators

In this study, a systematic evaluation was conducted to analyze the complex relationships among reliable phenotypic traits. The scatterplot presented in Fig. 9A illustrates the relationship between RWC and MSI, as well as other physiological indicators. RWC was positively correlated with F_V/F_M ($R^2 = 0.7$), MSI ($R^2 = 0.563$), and TChl ($R^2 = 0.383$) in Fig. 9, B, and C, respectively. There was a significant positive relationship between MSI with F_V/F_M ($R^2 = 0.669$) and a negative relationship with H_2O_2 ($R^2 = 0.608$) and SOD ($R^2 = 0.395$) in Fig. 9D, E, and F, respectively.

3.9. The results of path analysis

The results of the path analysis demonstrated that physiological, biochemical, and chlorophyll fluorescence traits played a strong and statistically significant role in explaining variation in the Copeland-based drought tolerance index (Table 3). The proposed model exhibited an exceptionally high explanatory power ($R^2 = 0.994$), and the low residual effect (0.0775) indicates that nearly all variation in the Copeland score was accounted for by the variables included in the model.

Among the evaluated traits, the F_M/F_0 ratio showed the highest total correlation with the Copeland score ($r_iY = 0.9682$) and the strongest positive direct effect ($P_i = 0.6218$), identifying it as the most influential determinant of drought tolerance. This trait also ranked first in the path analysis, and its high t-value (49.56) and strong statistical significance ($P < 0.001$) confirm its critical role in maintaining photosystem II (PSII) functional stability under DS.

The chlorophyll fluorescence parameters F_V/F_M and F_V/F_0 also exhibited high total correlations with the Copeland score (0.8990 and 0.8693, respectively); however, their contributions were predominantly mediated through indirect effects (0.8175 and 0.8383, respectively).

The RWC and PI_{ABS} likewise showed strong total correlations with the Copeland score (0.8526 and 0.8501, respectively) and substantial indirect effects. Although their direct effects were comparatively smaller, they remained statistically significant ($P < 0.001$), highlighting the importance of plant water status and photosynthetic performance in drought tolerance mechanisms.

Among the biochemical traits, MSI exhibited the highest positive direct effect after F_M/F_0 ($P_i = 0.1513$). In contrast, H_2O_2 and MDA showed strong negative correlations with the Copeland score, although their direct effects were not statistically significant in the path model.

The activities of antioxidant enzymes, including SOD and CAT, showed moderate positive correlations with the Copeland score, indicating their supportive role in drought tolerance, primarily through indirect pathways. Similarly, pigment-related traits such as TChl and carotenoids exhibited limited direct effects.

In complex biological models, a variance inflation factor (VIF) threshold of 10 is generally considered acceptable, whereas values below 5 are regarded as ideal. In the present study, all traits exhibited VIF values below 5, indicating the absence of severe multicollinearity and confirming the robustness and stability of the path analysis model.

3.10. D^2 statistics

The Mahalanobis D^2 analysis clearly differentiated walnut genotypes into three distinct clusters based on key drought-responsive traits (Table 4). Inter-cluster distances revealed substantial genetic divergence among clusters, with the greatest separation observed between clusters 1 and 2 ($D^2 = 7.51$), followed by clusters 2 and 3 ($D^2 = 5.78$), while the

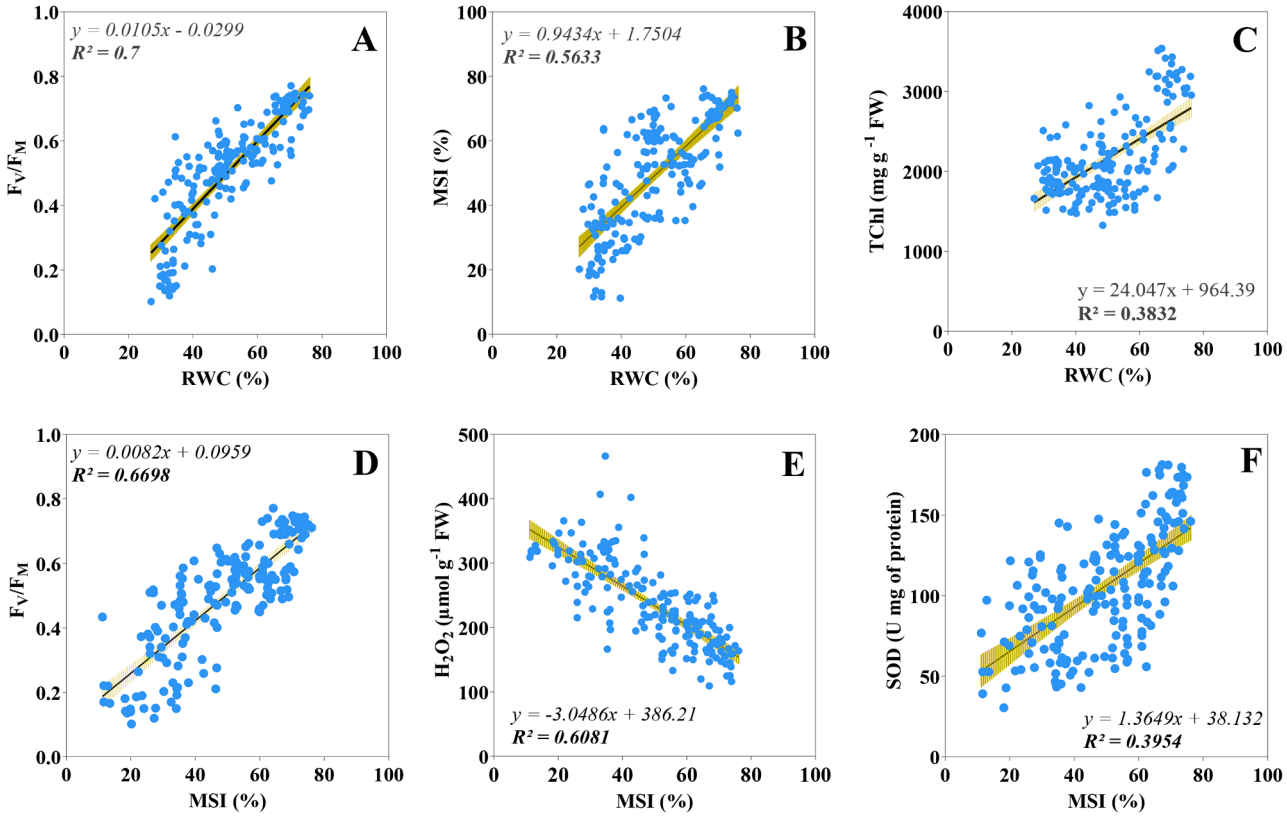

Fig. 9. Relationships between relative water contact (RWC) whit (A) maximum quantum yield of photosystem II (PSII) (F_V/F_M), (B) membrane stability index (MSI), (C) Total chlorophyll (TChl) and MSI with relationships between (D) F_V/F_M with (E) hydrogen peroxide (H_2O_2) (F). Superoxide dismutase (SOD) after 30 days under water stress. The coefficients of determination (R^2) of the relationships are given ($P < 0.01$).

Table 3
Path analysis of physiological, biochemical, and chlorophyll fluorescence traits contributing to Copeland-based drought tolerance ranking.

Trait	Total correlation with Copeland Score (r_iY)	Direct effect (P_i)	Indirect effect	Rank†	t-value	P-value	VIF
F_M/F_0	0.9682	0.6218	0.3463	1	49.56	<0.001	4.38
F_V/F_M	0.8990	0.0815	0.8175	2	5.32	<0.001	4.52
F_V/F_0	0.8693	0.0310	0.8383	3	2.42	0.016	4.55
RWC	0.8526	0.0542	0.7985	4	4.25	<0.001	4.52
PI_{ABS}	0.8501	0.0839	0.7662	5	6.07	<0.001	4.32
MSI	0.8178	0.1513	0.6664	6	11.35	<0.001	4.95
H_2O_2	−0.8116	−0.0130	−0.7985	7	−1.07	0.285	4.12
GB	0.7321	0.0087	0.7234	8	0.84	0.401	2.95
MDA	−0.7204	0.0188	−0.7392	9	1.85	0.066	2.88
SOD	0.6572	0.0210	0.6361	10	2.27	0.024	2.39
CAT	0.6519	0.0029	0.6490	11	0.30	0.766	2.70
TChl	0.6151	0.0545	0.5606	12	4.93	<0.001	3.39
TSC	0.6029	−0.0058	0.6087	13	−0.62	0.536	2.45
Carotenoids	0.5513	−0.0045	0.5558	14	−0.44	0.663	2.91
Proline	0.5098	0.0076	0.5022	15	0.95	0.343	1.78

Model statistics: $R^2 = 0.994$ | Residual effect = 0.0775.

Table 4
Mahalanobis D^2 statistics and comparative drought tolerance of walnut genotype clusters based on Copeland ranking.

A-Inter-cluster Mahalanobis D^2 distances among walnut genotypes based on key drought-responsive traits			
Cluster	1	2	3
1	0.000	7.5131	3.6811
2	7.5131	0.0000	5.7828
3	3.6811	5.7828	0.0000
B-Mean Copeland rank percentile across Mahalanobis D^2 clusters			
D^2 Cluster	Mean Rank Percentile†		
1	80.13		
2	**10.71**		
3	39.96		
†Lower percentile indicates higher drought tolerance.			
C-Statistical comparison of Copeland scores among D^2 clusters			
Test	Statistic	P-value	
Kruskal–Wallis	$H = 147.2043$	$\mathbf{1.0839 \times 10^{-32}}$	

Table 5
Stability assessment of Copeland-based drought tolerance ranking using Spearman's rank correlation.

Model	Value
Full Model	1.000000
Exclude ELECTRE	0.999472
Exclude SAW	0.999105
Exclude TOPSIS	0.999462
Exclude VIKOR	0.999196

smallest distance was detected between clusters 1 and 3 ($D^2 = 3.68$). These distances indicate pronounced multivariate differentiation among the identified groups (Table 4A). The mean Copeland rank percentile varied markedly across the Mahalanobis D^2 clusters. Cluster 2 exhibited the lowest mean rank percentile (10.71), indicating superior drought tolerance among genotypes assigned to this cluster. In contrast, cluster 1 showed the highest mean rank percentile (80.13), reflecting relatively lower drought tolerance, whereas cluster 3 displayed an intermediate response with a mean percentile of 39.96 (Table 4 B). A nonparametric comparison of Copeland scores among clusters using the Kruskal–Wallis test confirmed statistically significant differences between the Mahalanobis D^2 clusters ($H = 147.20$, $P = 1.08 \times 10^{-32}$) (Table 4 C). This result demonstrates that the multivariate clustering based on drought-responsive traits was strongly associated with differences in Copeland-based drought tolerance ranking among walnut genotypes.

3.11. Stability analysis

The stability analysis based on Spearman rank correlation coefficients demonstrated an exceptionally high level of consistency in genotype ranking across all model configurations (Table 5). The Copeland-based ranking derived from the full model showed an almost perfect agreement with rankings obtained after sequential exclusion of individual MCDM methods. Specifically, the rank correlation remained extremely high when ELECTRE ($\rho = 0.99947$), SAW ($\rho = 0.99911$), TOPSIS ($\rho = 0.99946$), or VIKOR ($\rho = 0.99920$) was excluded from the model. These results indicate that the overall drought tolerance ranking was remarkably robust and insensitive to the removal of any single decision-making method, confirming the high stability and reliability of the integrated ranking framework.

3.12. Stability across validation of genotypes

The results presented in Table 6 illustrate the stability of the ranking of the top ten genotypes across different model validation scenarios, including the full model and the exclusion of each MCDM method (ELECTRE, SAW, TOPSIS, and VIKOR). Overall, a very high level of agreement among rankings was found across all scenarios, indicating strong robustness of the multi-criteria decision-making process and high reliability of the genotype selection framework. Genotypes Ke16 and KeSh9 consistently retained the first and second ranks, respectively, across all validation scenarios without any change, demonstrating their stable superiority regardless of the decision-making method applied. Similarly, genotype Ke18 exhibited high ranking stability, maintaining the third position or showing only minor fluctuations (between ranks 3 and 4), which reflects a strong consensus among the different MCDM methods in identifying superior genotypes. Moderate-ranked genotypes such as Fa15, Fa16, and KhR5 displayed only limited rank variations, with most shifts occurring within a narrow range of one to two positions. These minor changes suggest that while differences in weighting

Table 6
Stability of the top 10 genotype rankings across different MCDM validation scenarios.

Genotype	Full Model	Exclude ELECTRE	Exclude SAW	Exclude TOPSIS	Exclude VIKOR
Ke16	1	1	1	1	1
KeSh9	2	2	2	2	2
Ke18	3	3	4	3.5	3
Fa15	4	5	5	5	6
Fa16	5	4	6	6	5
KhR5	6	6	7	3.5	4
Ke20	7	7.5	3	8	9
Ku8	8	7.5	8	9	7.5
KeSh8	9	9	9	7	7.5
KhR4	10	10	11.5	10	10

schemes and ranking logic among MCDM methods may slightly influence their relative positions, their overall classification among the top-performing genotypes remains stable. In contrast, genotypes including Ke20, Ku8, and KeSh8 exhibited the largest rank fluctuations across validation scenarios, particularly when specific methods were excluded, resulting in more noticeable changes in their relative rankings. Nevertheless, these genotypes consistently remained within the top ten, indicating acceptable stability in their overall multi-trait performance. In summary, the results demonstrate that the final genotype rankings show considerable robustness to the exclusion of individual decision-making methods. The highest-ranked genotypes, in particular, maintained their positions consistently across all scenarios, thereby confirming the strong validity and reliability of the integrated framework employed in this study for identifying stable and superior genotypes.

4. Discussion

Walnut trees exposed to environmental stresses, including drought, activate a complex network of signaling pathways (Habibi et al., 2024). Numerous studies have highlighted the importance of relative water content (RWC) as a physiological biomarker of drought stress (DS) in fruit and nut trees, including walnut (Arab et al., 2023). Our results showed a decrease in RWC in most genotypes after genotypes were subjected to DS. Knipfer et al. (2020) reported that the reduction in water content in walnut trees is linked to impaired root growth and stomatal regulation. Sadat-Hosseini et al. (2019) also explained how walnut roots behave under DS. Water stress severely damages plant growth and disrupts various physiological and biochemical processes, which aligns with the observations of Karami et al. (2018) and Habibi et al. (2024). Another resistance mechanism in drought-tolerant plants involves stomatal closure through an ABA-dependent pathway, which reduces water loss (Arab et al., 2020).

It is well-established that metabolic processes, such as the accumulation of proline and carbohydrates, play a key role in the adaptation of fruit trees to environmental stresses (Lotfi et al., 2019; Lotfi et al., 2009; Habibi et al., 2024). Several studies have shown that osmotic regulators involved in DS metabolism serve as an energy source, which is crucial for utilizing energy produced during photosynthesis (Knipfer et al., 2020). Arab et al. (2023) suggested that osmotic regulation may be a key mechanism in the response of Persian walnut to DS. In line with these findings, our study showed significant increases in osmoregulatory compounds such as total soluble carbohydrates (TSC), proline, and glycine betaine (GB) in stressed genotypes compared to controls. We also observed a wide range of variation in walnut response to DS. The diverse phenotypic responses of this local Persian walnut genetic resource in our common garden study likely reflect the genetic variability in responses reported by Arab et al. (2023). Furthermore, the role of osmotic regulators such as TSC, proline, and GB varies. For instance, TSC and GB play significant roles in increasing osmotic potential and turgor pressure, while proline helps balance osmotic pressure and improve cellular membrane fluidity (Lehr et al., 2022; Momayyezi et al., 2025; Farajpour, 2025b).

Another metabolic pathway involved in the DS response is signaling and the accumulation of reactive oxygen species (ROS), including hydrogen peroxide (H_2O_2). We observed diverse responses among genotypes to DS in terms of H_2O_2 accumulation. High ROS levels negatively affect cellular protection and membrane stability (Aliniaeifard et al., 2020). H_2O_2 accumulation induced by DS directly damages photosystem II (PSII) and its subunits or inhibits protein resynthesis and PSII repair (Ru et al., 2023). This leads to increased ion leakage and excessive production of malondialdehyde (MDA). The accumulation of H_2O_2 and MDA followed a parallel trend, as indicated by the strong positive correlation between H_2O_2 and MDA (Fig. 8A). Moreover, there was a significant negative correlation between the membrane stability index (MSI) and both H_2O_2 and MDA, suggesting severe damage to the cellular membrane. Water stress induced high levels of H_2O_2, MDA, and electrolyte leakage, which were associated with increased activity of antioxidant enzymes, including SOD (Mostakhdemi et al., 2022). This suggests that lipid peroxidation of membrane lipids was more pronounced under severe stress conditions. Additionally, the linear regression model showed that maintaining membrane stability was a function of higher levels of SOD, higher RWC, and lower H_2O_2 levels (Fig. 10). These results suggest that genotypes with higher levels of SOD have higher amounts of MSI. Plants increase the activity of antioxidant enzymes to maintain ROS balance and reduce stress-induced damage. In this study, SOD levels increased significantly, and the enhanced production of SOD in tolerant genotypes contributed to membrane fluidity and reduced water loss by scavenging H_2O_2.

A common indicator of DS is the reduction in chlorophyll content. Structural damage to photosynthetic centers, destruction of chloroplasts, and oxidative stress are key factors contributing to the decline in plant pigments (Ru et al., 2023). According to ROC curve analysis, plant pigment-related parameters exhibited high area under the curve (AUC) values, with the highest Youden Index (YI) observed for total chlorophyll (TChl) content. Additionally, we observed a wide range of phenotypic differences in TChl content among local genotypes under DS. A severe reduction in TChl content may be attributed to genotype sensitivity as well as the activity of degrading enzymes like chlorophyllase (Abubakar et al., 2023; Shtai et al., 2024). We also found a positive correlation between TChl content and RWC as well as photosynthetic performance-related traits (Fig. 8). Moreover, DS can lead to leaf senescence or chlorosis due to a decrease in chlorophyll levels, which subsequently disrupts photosystem II (Habibi et al., 2024). Drought stress has been shown to impair chlorophyll biosynthesis pathways while simultaneously accelerating chlorophyll degradation, leading to a net decline in TChl, particularly in drought-sensitive walnut genotypes (Lotfi et al., 2019). In walnut, reduced TChl under water deficit has been associated with damage to thylakoid membranes and destabilization of pigment–protein complexes within the photosynthetic apparatus (Kalaji et al., 2017). Maintenance of higher chlorophyll levels under drought conditions is considered a key adaptive trait, as it reflects the ability of genotypes to preserve chloroplast structural integrity and delay stress-induced senescence (Arab et al., 2023). Moreover, chlorophyll stability under drought has been linked to improved antioxidant capacity, which protects pigments from oxidative degradation caused by excess ROS (Momayyezi et al., 2025; Pileh et al., 2025). Genotypes capable of sustaining higher TChl content under DS generally exhibit enhanced light-harvesting efficiency and greater photosynthetic resilience, contributing to improved carbon assimilation under limited water availability (Knipfer et al., 2020; Arab et al., 2023). Therefore, variation in TChl among walnut genotypes under DS represents a meaningful physiological indicator of differential drought tolerance and adaptive potential (Habibi et al., 2024).

Linear regression analysis revealed that the stability of F_V/F_M in drought-tolerant genotypes was a function of higher RWC and MSI. Interestingly, higher chlorophyll content played a significant role in preventing the decline of F_V/F_M (Fig. 9C). We also found a significant positive correlation between RWC and MSI, and TChl (Fig. 9), indicating that genotypes with higher levels of these compounds performed better in maintaining RWC. Our results indicate that the ability to maintain chlorophyll content and relative water content contributes to drought adaptation and inhibits the reduction of F_V/F_M in resistant walnut genotypes. The results of the ROC curve analysis illustrated that the carotenoid index is a reliable marker for selecting superior genotypes under DS. It has been reported that carotenoids are synthesized in plastids under DS and act as antioxidants by neutralizing ROS (Liu et al., 2019; Aliniaeifard et al., 2020). Moreover, carotenoids can contribute to stomatal closure, reduced transpiration, and the regulation of stress-responsive genes through the activation of ABA (Petrozza et al., 2023; Sohail et al., 2025). In our study, a significant positive correlation was observed between carotenoids with TChl, SOD, and CAT. Additionally, carotenoids may function as retrograde signals, enhancing

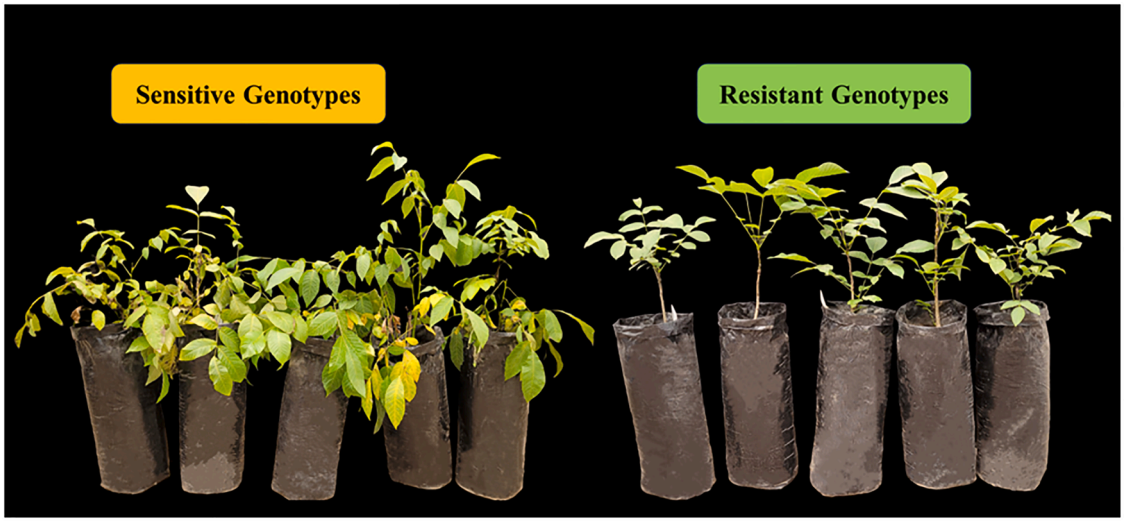

Fig. 10. Appearance and health of drought-sensitive and drought-tolerant Persian walnut genotypes under drought stress.

drought tolerance by protecting cell membranes and improving photosynthesis, an effect that is more pronounced in drought-tolerant genotypes (Gorni et al., 2025).

Among various biological pathways, photosynthesis processes and cell growth are among the most sensitive aspects of plant responses to environmental stresses (Habibi et al., 2024). Our results showed significant effects on nearly all parameters derived from the OJIP test under DS. This finding is consistent with previous studies on Persian walnut (Arab et al., 2023). The ROC curve analysis identified key indicators that reflect the most critical points of damage under DS and recovery conditions. The role of ROC curves in selecting the best indices is to assess their accuracy and ability to differentiate between sensitive and resistant genotypes. The ROC curve, F_V/F_M and PI_{ABS} were identified as key indicators with the highest AUC and YI rankings, respectively, highlighting their significance in reflecting the effects of DS on ETC= (Table 1).

The OJIP fluorescence transient pattern, comprising the O, J, I, and P phases, reflects the oxidation and reduction states of photosystems (Strasser et al., 2004). Chlorophyll fluorescence intensity serves as an indicator of thylakoid membrane integrity and the efficiency of electron transfer from Photosystem II (PSII) to Photosystem I (PSI). In this study, chlorophyll fluorescence analysis was employed as a rapid and non-destructive method to evaluate the performance of the photosynthetic apparatus after 30 days of DS. Photosynthetic parameters were measured under normal irrigation and DS conditions in Iranian walnut genotypes to identify physiological indices associated with photosynthesis. Our results revealed significant phenotypic variation among genotypes in traits related to chlorophyll fluorescence. In walnut trees, one of the primary physiological effects of DS is the disruption of the photosynthetic process (Momayyezi et al., 2022; Habibi et al., 2024). Drought stress induces stomatal closure, limits carbon availability at carboxylation sites in chloroplasts, and consequently overexcites the photosynthetic apparatus, particularly PSII (Kalaji et al., 2017; Momayyezi et al., 2025).

The results of the OJIP test in this study demonstrated that DS significantly inhibits the electron transfer activities of PSII. Based on our findings, the reduction in F_V/F_M, as well as F_V/F_0 and F_M/F_0, under DS conditions particularly in drought-sensitive genotypes reflects the accumulation of QA, indicating a blockage in electron transfer from QA to QB on the acceptor side of PSII, as reported by Kalaji et al. (2017). F_M/F_0 represents the first stage of light energy conversion in the electron transport chain and indicates the relative maximum and minimum chlorophyll fluorescence values (Kalaji et al., 2017). A decrease in F_M/F_0 and F_V/F_M suggests a reduction in the quantum yield of photochemistry in PSII, disrupting the photosynthetic apparatus, which reflects the energy flow from the water-splitting site (Kalaji et al., 2017).

In addition to the inhibition of electron transfer from QA to QB, DS disrupts the connectivity among PSII units, thereby reducing overall energy transfer efficiency and electron flow beyond QA (Strasser et al., 2004). These disturbances are reflected in OJIP fluorescence kinetics as an enhanced J-step and a weakened I–P phase, indicating over-reduction of the plastoquinone pool and restricted electron transfer to downstream carriers under severe water deficit conditions (Zhou et al., 2019). Furthermore, drought-induced deactivation of reaction centers and impaired energetic connectivity between PSII and PSI lead to a decline in overall electron transport efficiency and reduced energy fluxes per cross-section (Kalaji et al., 2017). Under prolonged DS, limitations in QA^- re-oxidation increase susceptibility to photoinhibition and promote non-photochemical energy dissipation (NPQ) as a protective response. In contrast, drought-tolerant genotypes tend to enhance alternative electron pathways, including cyclic electron flow around PSI, which contributes to ATP generation and photoprotection when linear electron flow is constrained (Arab et al., 2023). Collectively, these findings highlight the value of comprehensive OJIP analysis for detecting subtle functional impairments in the photosynthetic electron transport chain that cannot be captured by single fluorescence ratios. Previous studies have also reported that F_V/F_M is a valuable biophysical marker for screening plants under environmental stresses (Arab et al., 2023). The indices identified by the ROC curve in this study, particularly F_V/F_M, represent water splitting, the structural integrity of PSII, and quantum yield efficiency, offering insights into how water disrupts electron transport and affects photosynthetic performance.

Additionally, The PI_{ABS} is considered one of the most integrative and sensitive chlorophyll fluorescence parameters for evaluating PSII performance under environmental stress conditions. Unlike single fluorescence ratios, PI_{ABS} provides a comprehensive assessment of photosynthetic functioning by simultaneously integrating energy absorption, excitation trapping efficiency, and the subsequent conversion of trapped energy into electron transport. Consequently, PI_{ABS} has been widely used as a robust indicator of plant stress tolerance across a broad range of species and stress conditions, including drought, salinity, and extreme temperatures (Arab et al., 2023).

In the present study, DS induced significant and genotype-dependent changes in PI_{ABS} among native walnut genotypes, reflecting substantial variability in PSII stability and photosynthetic resilience under water-limited conditions. The observed reduction in PI_{ABS} under DS indicates impairments in electron transport capacity and disruptions in the functional integrity of PSII reaction centers, which are commonly

associated with drought-induced photoinhibition and increased oxidative stress. However, the magnitude of PI_{ABS} decline varied markedly among genotypes, indicating differential abilities to maintain efficient energy fluxes and protect the photosynthetic apparatus under stress conditions (Kalaji et al., 2017). Genotypes that maintained higher PI_{ABS} values under DS likely possess more effective photoprotective mechanisms, such as enhanced dissipation of excess excitation energy, improved maintenance of reaction center openness, and more efficient electron transport chains (Zuo et al., 2025). These physiological advantages enable sustained photosynthetic activity and carbon assimilation despite reduced water availability, ultimately contributing to enhanced drought tolerance, whereas genotypes exhibiting sharp declines in PI_{ABS} appear more sensitive and more vulnerable to stress-induced photosynthetic impairment and oxidative damage. The present findings are consistent with those reported by Arab et al. (2023) in walnut. The strong association observed between PI_{ABS} and drought tolerance ranking in this study further emphasizes the value of this index as a reliable screening criterion for identifying drought-tolerant walnut genotypes. Given its integrative nature and high sensitivity to stress-induced alterations in photosynthetic performance, PI_{ABS} provides valuable insights into genotype-specific adaptive strategies and can serve as an effective selection indicator in breeding programs aimed at improving drought resistance. Moreover, Habibi et al. (2024) stated that, aside from F_V/F_M, the indices PI_{ABS} significantly decrease under heat, water, and combined stresses.

Based on the DS scoring index, the degree of wilting, leaf shedding in walnut genotypes, and the drought sensitivity index increased (data not shown). The results of the present study revealed that at the end of the DS period, resistant genotypes exhibited less wilting and leaf shedding, consistent with previous research on walnuts (Vahdati et al., 2009; Arab et al., 2023). The findings indicated substantial phenotypic variation across the studied traits. With increasing DS intensity, the RWC of leaves, particularly in sensitive walnut genotypes, decreased, leading to leaf wilting. The primary cause of this response is the shortage of soil water and the reduced rate of water transport from the soil to aerial plant parts. Furthermore, a decline in RWC can elevate the levels of reactive oxygen species (ROS) in tissues, resulting in a reduction in the membrane stability index (MSI). ROS contribute to a decrease in chlorophyll content by inhibiting its synthesis, causing structural damage to photosystem centers, disrupting chloroplasts, or enhancing the activity of chlorophyll-degrading enzymes, such as chlorophyllase (Karimi et al., 2018; Habibi et al., 2024). Consequently, leaves initially turn yellow, the plant loses its photosynthetic capacity, and ultimately, leaf shedding occurs. As shown in Fig. 8, drought-tolerant Iranian walnut genotypes appeared visually healthy, indicating that these three indices are suitable for screening drought-tolerant genotypes.

This phenomenon indicates that leaf characteristics may be more significantly affected by DS and can serve as reliable indicators of drought tolerance in walnuts. These findings align with previous studies (Arab et al., 2023). Under DS conditions, photosynthesis may be inhibited due to leaf chlorosis and stomatal closure. As a result, stomatal closure suppresses the activity of the Rubisco enzyme, and it has a lesser impact on increasing transpiration, ultimately leading to reduced carbohydrate reserves, decreased growth rates, and accelerated plant senescence (Arab et al., 2020; Habibi et al., 2024). Additionally, a wide range of morphological characteristics and responses to DS were observed among the studied genotypes. In the present study, significant differences were noted among most drought-tolerant genotypes, with smaller plant size and small, narrow leaves being notable visual characteristics. However, in some cases, vigorous genotypes also exhibited high drought tolerance.

The genotypes examined in this experiment were collected from a diverse range of climatic conditions, including hot and arid regions such as Kerman and Khorasan, cold and high-precipitation areas like Zanjan and Chaharmahal and Bakhtiari, and cold regions such as Kurdistan. This climatic diversity resulted in a broad spectrum of responses in the measured traits (Fig. 2). Arab et al. posited that climatic factors, particularly temperature (in the coldest month and season) and precipitation (in the driest and hottest seasons), are key determinants of drought tolerance in Iranian walnut genotypes. In this context, these researchers noted that the identified drought-tolerant genotypes were genotypes derived from mother trees that had adapted over many years to the climatic conditions of hot and arid regions as well as cold regions. The results of this study revealed that drought-tolerant genotypes were present across all sampled provinces, which is consistent with the findings of Arab et al. (2020)), (2023).

5. Conclusion

This study underscores the remarkable genetic and phenotypic diversity among Iranian walnut genotypes in response to DS, highlighting their substantial potential for breeding drought-tolerant rootstocks. The evaluation of 183 diverse walnut genotypes based on physiological, photosynthetic, and biochemical traits revealed that drought-tolerant genotypes exhibit reduced wilting and leaf shedding, with minimal declines in relative water content, alongside more active antioxidant and osmotic regulatory mechanisms. Using ROC curve analysis and the AUC and YI algorithms, traits such as F_V/F_M, PI_{ABS}, TChl, and carotenoids were identified as reliable markers for screening drought-tolerant genotypes. Additionally, optimal threshold values for the evaluated traits in response to DS were reported for different walnut genotypes. This study provides a precise phenotyping framework that lays the foundation for the development of drought-tolerant walnut cultivars. Moreover, the integration of multi-criteria ranking methods, particularly the Copeland aggregation approach, provides breeders with a robust and highly effective tool, significantly enhancing the accuracy and efficiency of selecting resistant genotypes in walnut breeding programs. The rankings derived from GMCDM methods, combined with the Copeland approach, identified superior genotypes such as Ke16, KeSH9, and Ke18 as optimal candidates. These findings emphasize the critical role of climatic adaptation in shaping drought tolerance and demonstrate that tolerant walnut genotypes from diverse Iranian regions represent a valuable genetic resource for enhancing the species' resilience to drought and changing climatic conditions. Furthermore, the obtained results require further validation under field conditions and across multiple growing seasons to confirm the stability of genotype responses to DS to strengthen the generalizability of the findings. In addition, the incorporation of the identified superior genotypes into breeding programs, particularly as drought-tolerant rootstocks, could play a significant role in improving walnut yield performance and production stability under variable climatic conditions. The integration of these findings with molecular and genetic data in future studies will facilitate the development of new drought-tolerant cultivars. Overall, the results of this study provide a practical framework for the sustainable breeding and management of walnut in arid and semi-arid regions.

Funding

No funding.

CRediT authorship contribution statement

Asaad Habibi: Writing – original draft, Validation, Software, Project administration, Methodology, Investigation, Formal analysis, Data curation, Conceptualization. **Mohammad Soltani:** Software, Formal analysis. **Saadat Sarikhani:** Writing – review & editing, Supervision, Project administration. **Mahmoud Reza Roozban:** Writing – review & editing. **Adamo Domenico Rombolà:** Writing – review & editing. **Mohammad Hassan Jafari Sayadi:** Writing – review & editing. **Kourosh Vahdati:** Writing – review & editing, Supervision, Project administration.

Declaration of competing interest

The authors declare that they have no known competing financial interests or personal relationships that could have appeared to influence the work reported in this paper.

Acknowledgement

We would like to thank the Iran National Science Foundation (INSF), Center of Excellence for Walnut Improvement and Technology of Iran, and the University of Tehran for their support.

Data availability

Data will be made available on request.

References

Abubakar, A.S., Wu, Y., Chen, F., Zhu, A., Chen, P., Chen, K., Qiu, X., Huang, X., Zhao, H., Chen, J., Gao, G., 2023. Comprehensive analysis of WUSCEL-related homeobox gene family in Ramie (Boehmeria nivea) indicates its potential role in adventitious root development. Biology 12 (12), 1475.

Aliniaeifard, S., et al., 2014. Stomatal malfunctioning under low VPD conditions: induced by alterations in stomatal morphology and leaf anatomy or in the ABA signaling? Physiol. Plant Biol. 152, 688–699.

Aliniaeifard, S., Maleki Asayesh, Z., Driver, J., Vahdati, K., 2020. Stomatal features and desiccation responses of Persian walnut leaf as caused by in vitro stimuli aimed at stomatal closure. Trees 34, 1219–1232.

Arab, M.M., et al., 2020. Combining phenotype, genotype, and environment to uncover genetic components underlying water use efficiency in Persian walnut. J. Exp. Bot. 71, 1107–1127.

Arab, M.M., et al., 2023. Natural variation in photosynthesis and water use efficiency of locally adapted Persian walnut populations under drought stress and recovery. Plant Physiol. Biochem. 201, 107859.

Bates, L.S., Waldren, R.P., Teare, I.D., 1973. Rapid determination of free proline for water-stress studies. Plant Soil 39 (1), 205–207.

Cakmak, I., Marschner, H., 1992. Magnesium deficiency and high light intensity enhance activities of superoxide dismutase, ascorbate peroxidase, and glutathione reductase in bean leaves. Plant Physiol. 98 (4), 1222–1227.

Chatrabnous, N., Arzani, K., Sarikhani, S., Pavan, S., 2024. Phenotypic and pomological diversity of selected native walnut (*Juglans regia*) populations: implications for breeding and cultivation programs. Euphytica 220 (7), 98.

de-Matos Lessa, M.S.C., Amaral, T.M., Leão, P.C.S., Oliva, J.T., 2024. Multi-criteria decision analysis applied to Brazilian grapevine genotype selection. J. Food Compos. Anal. 130, 106126.

Dragincic, J., Korac, N., Blagojevic, B., 2015. Group multi-criteria decision making (GMCDM) approach for selecting the most suitable table grape variety intended for organic viticulture. Comput. Electron. Agric. 111, 194–202.

Dubois, M., Gilles, K.A., Hamilton, J.K., Rebers, P.A., Smith, F., 1956. Colorimetric method for determination of sugars and related substances. Anal. Chem. 28 (3), 350–356.

Farajpour, M., 2025a. Fate of pistachio production in Iran holds lessons for the world. Nature 639 (8054), 306-306.

Farajpour, M., 2025b. Synergizing genetic algorithms and neural networks to decode mineral-antioxidant dynamics in black-raspberry. Ind. Crops Prod. 232, 121266.

Figueira, J., Greco, S., Ehrgott, M., 2013. Multiple Criteria Decision Analysis: State of the Art Surveys. Springer Science & Business Media.

Fluss, R., Faraggi, D., Reiser, B., 2005. Estimation of the Youden Index and its associated cutoff point. Biom. J. 47 (4), 458–472.

Fridovich, I., 1986. Superoxide dismutases. In: Advances in Enzymology and Related Areas of Molecular Biology, 58. Academic Press, pp. 61–97.

Gorni, P.H., Rodrigues, C., Spera, K.D., Correia, R.F.C.C., Mendes, N.A.C., Dos Reis, A.R., 2025. Selenium fertilization enhances carotenoid and antioxidant metabolism to scavenge ROS and increase yield of maize plants under drought stress. Plant Physiol. Biochem. 221, 109675.

Grieve, C.M., Grattan, S.R., 1983. Rapid assay for determination of water-soluble quaternary-amino compounds. Plant Soil 70, 303–307.

Guiqing, X., Jinyao, L., Haifang, H., Tuqiang, C., 2024. Effect of deficit irrigation on physiological, morphological and fruit quality traits of six walnut tree cultivars in the inland area of Central Asia. Sci. Hortic. 329, 112951.

Habibi, A., Hamedpour-Darabi, M., Vahdati, K., 2022. Local cultural values of Persian walnut in Iran. The Cultural Value of Trees. Routledge, pp. 162–173.

Habibi, A., Sarikhani, S., Arab, M.M., Soltani, M., Aliniaifard, S., Roozban, M.R., Vahdati, K., 2024. Drought and heat stress interactions: unveiling the molecular and physiological responses of Persian walnut. Plant Physiol. Biochem. 217, 109237.

Habibi, A., Sarikhani, S., Arab, M.M., Soltani, M., Rombola, A.D., Roozban, M.R., Vahdati, K., 2025. Combined drought and heat stress intensifies antioxidant responses and gene expression in Persian walnut (*Juglans regia* L.). BMC Plant Biol.

Hanley, J.A., McNeil, B.J., 1982. The meaning and use of the area under a receiver operating characteristic (ROC) curve. Radiology 143 (1), 29–36.

Harris, C.R, Millman, K.J, van der Walt, S.J, Gommers, R, Virtanen, P, Cournapeau, D, Wieser, E, Taylor, J, Berg, S, Smith, N.J, Kern, R., Picus, M., Hoyer, S., van Kerkwijk, M.H., Brett, M., Haldane, A., Del Río, J.F., Wiebe, M., Peterson, P., Gérard-Marchant, P., Sheppard, K., Reddy, T., Weckesser, W., Abbasi, H., Gohlke, C., Oliphant, T.E., 2020. Array programming with NumPy. Nature 585 (7825), 357–362.

Hassani, D., Sarikhani, S., Dastjerdi, R., Mahmoudi, R., Soleimani, A., Vahdati, K., 2020. Situation and recent trends on cultivation and breeding of Persian walnut in Iran. Sci. Hortic. 270, 109369.

Heath, R.L., Packer, L., 1968. Photoperoxidation in isolated chloroplasts: I. Kinetics and stoichiometry of fatty acid peroxidation. Arch. Biochem. Biophys. 125 (1), 189–198.

Heidarzadeh, S., Pourdarbani, R., Zadvali, F., Pashazadeh, A., 2020. Evaluating and ranking the development level of rural areas of Tabriz using Copeland model and comparison the results with TOPSIS, VIKOR and ELECTRE models. Yuz. Yıl Univ. J. Agric. Sci. 30 (3), 498–509.

Huang, J., Ling, C.X., 2005. Using AUC and accuracy in evaluating learning algorithms. IEEE Trans. Knowl. Data Eng. 17 (3), 299–310.

Hwang, C.L., Yoon, K., 1981. Multiple Attribute Decision Making: Methods and Applications. Springer-Verlag.

Kalaji, H.M., et al., 2017. Frequently asked questions about chlorophyll fluorescence, the sequel. Photosynth. Res. 132, 13–66.

Karimi, S., Karami, H., Mokhtassi-Bidgoli, A., Tavallali, V., Vahdati, K., 2018. Inducing drought tolerance in greenhouse grown Juglans regia by imposing controlled salt stress: the role of osmotic adjustment. Sci. Hortic. 239, 181–192.

Knipfer, T., Bambach, N., Hernandez, M.I., Bartlett, M.K., Sinclair, G., Duong, F., Kluepfel, D.A., McElrone, A.J., 2020. Predicting stomatal closure and turgor loss in woody plants using predawn and midday water potential. Plant Physiol. 184 (2), 881–894.

Kouhi, M., Rezaei, A., Hassani, D., Sarikhani, S., Vahdati, K., 2020. Phenotypic evaluation and identification of superior Persian walnut (*Juglans regia* L.) genotypes in Mazandaran province, Iran. J. Nuts 11 (4), 315–326.

Lehr, P.P., Hernández-Montes, E., Ludwig-Müller, J., Keller, M., Zörb, C., 2022. Abscisic acid and proline are not equivalent markers for heat, drought and combined stress in grapevines. Aust. J. Grape Wine Res. 28 (1), 119–130.

Li, J., 2024. Area under the ROC Curve has the most consistent evaluation for binary classification. PLoS ONE 19 (12), e0316019.

Lichtenthaler, H.K., 1987. Chlorophylls and carotenoids: pigments of photosynthetic biomembranes. In: Methods in Enzymology, 148. Academic Press, pp. 350–382.

Liu, T., Luo, T., Guo, X., Zou, X., Zhou, D., Afrin, S., Li, G., Zhang, Y., Zhang, R., Luo, Z., 2019. PgMYB2, a MeJA-responsive transcription factor, positively regulates the dammarenediol synthase gene expression in *Panax ginseng*. Int. J. Mol. Sci. 20 (9), 2219.

Loreto, F., Velikova, V., 2001. Isoprene produced by leaves protects the photosynthetic apparatus against ozone damage, quenches ozone products, and reduces lipid peroxidation of cellular membranes. Plant Physiol. 127 (4), 1781–1787.

Lotfi, N., Vahdati, K., Kholdebarin, B., Amiri, R., 2009. Soluble sugars and proline accumulation play a role as effective indices for drought tolerant screening in Persian walnut (*Juglans regia* L.) during germination. Fruits 65 (2), 1–14.

Lotfi, N., Soleimani, A., Vahdati, K., Çakmakçı, R., 2019. Comprehensive biochemical insights into the seed germination of walnut under drought stress. Sci. Hortic. 250, 329–343.

Madanchian, M., Taherdoost, H., 2023. A comprehensive guide to the TOPSIS method for multi-criteria decision making. Sustain. Soc. Dev. 1 (1), 2220.

McKinney, W., 2010. Data structures for statistical computing in Python. In: Proceedings of the 9th Python in Science Conference, pp. 56–61.

Momayyezi, M., Rippner, D.A., Duong, F.V., Raja, P.V., Brown, P.J., Kluepfel, D.A., Earles, J.M., Forrestel, E.J., Gilbert, M.E., McElrone, A.J., 2022. Structural and functional leaf diversity lead to variability in photosynthetic capacity across a range of *Juglans regia* genotypes. Plant Cell Environ. 45 (8), 2351–2365.

Momayyezi, M., Knipfer, T., Hernandez-Perez, M.I., Kluepfel, D.A., Wakholi, C., Rippner, D.A., Albuquerque, C.P., Bambach, N.E., DeGrom, J., McElrone, A.J., 2025. Differential impact of commercial rootstocks on the physiological response of a common walnut scion to drought stress. Physiol. Plant. 177 (2), e70188.

Mu, Q., et al., 2021. The physiological response of winter wheat under short-term drought conditions and the sensitivity of different indices to soil water changes. Agric. Water Manag. 243, 106475.

Opricovic, S., Tzeng, G.H., 2004. The compromise solution by MCDM methods: a comparative analysis of VIKOR and TOPSIS. Eur. J. Oper. Res. 156 (2), 445–455.

Opricovic, S., 1998. Multicriteria Optimization of Civil Engineering Systems. Faculty of Civil Engineering, Belgrade.

Pedregosa, F., Varoquaux, G., Gramfort, A., Michel, V., Thirion, B., Grisel, O., Blondel, M., Prettenhofer, P., Weiss, R., Dubourg, V., Vanderplas, J., 2011. Scikit-learn: machine learning in Python. J. Mach. Learn. Res. 12, 2825–2830.

Petrozza, A., Summerer, S., Melfi, D., Mango, T., Vurro, F., Bettelli, M., Janni, M., Cellini, F., Carriero, F., 2023. A lycopene ε-cyclase TILLING allele enhances lycopene and carotenoid content in fruit and improves drought stress tolerance in tomato plants. Genes 14 (6), 1284.

Pileh, F., Ebadi, A., Zamani, Z., Babalar, M., Climent, M.F.L., Habibi, A., 2025. Improving salt stress tolerance in grapevine rootstocks and cultivars through foliar application of ascorbic acid. Sci. Rep. 15 (1), 41860.

Robin, J., Bernard, A., Albouy, L., Papillon, S., Tranchand, E., Hebrard, M.N., Philibert, J. B., Barbedette, M., Schafleitner, S., Wenden, B., Barreneche, T., 2024. Description of phenological events of persian walnut (*Juglans regia* L.) according to the extended BBCH scale and historical scales. Horticulturae 10 (4), 402.

Roy, B., 1991. The outranking approach and the foundations of ELECTRE methods. In: Bana e Costa, C.A. (Ed.), Readings in Multiple Criteria Decision Aid. Springer, pp. 155–183.
Ru, C., Hu, X., Chen, D., Wang, W., Zhen, J., Song, T., et al., 2023. Individual and combined effects of heat and drought and subsequent recovery on winter wheat (*Triticum aestivum* L.) photosynthesis, nitrogen metabolism, cell osmoregulation, and yield formation. Plant Physiol. Biochem. 196, 222–235.
Saari, D.G., Merlin, V.R., 1996. The Copeland method: I.: relationships and the dictionary. Econ. Theory 8 (1), 51–76.
Sadat-Hosseini, M., Vahdati, K., Boroomand, N., Arab, M.M., Asadi-Yekta, S., 2019. How walnut roots respond to drought stress: a morphological and anatomical study. *South-Western Journal of Horticulture*. Biol. Environ. 10 (2), 51–64.
Seabold, S., Perktold, J., 2010. Statsmodels: econometric and statistical modeling with python. SciPy 7 (1), 92–96.
Shan, G., 2015. Improved confidence intervals for the Youden Index. PLoS ONE 10 (7), e0127272.
Shtai, W., et al., 2024. Soil water availability modulates the response of grapevine leaf gas exchange and PSII traits to a simulated heat wave. Plant Soil 1–18.
Sohail, H., Noor, I., Hussain, H., Zhang, L., Xu, X., Chen, X., Yang, X., 2025. Genome editing in horticultural crops: augmenting trait development and stress resilience. Hortic. Plant J.
Strasser, R.J., Tsimilli-Michael, M., Srivastava, A., 2004. Analysis of the chlorophyll a fluorescence transient. Chlorophyll a Fluorescence: A Signature of Photosynthesis. Springer, Netherlands, Dordrecht, pp. 321–362.
Taherdoost, H., 2023. Analysis of simple additive weighting method (SAW) as a multi attribute decision-making technique: a step-by-step guide. J. Manag. Sci. Eng. Res. 6 (1), 21–24.
Taheri, A., Seyedi, N., Abdollahi Mandoulakani, B., Miraghaderi, Gh., Najafi, S., Vahdati, K., Sahin, M., Hatterman-Valenti, H., Kaya, O., 2026. Genetic diversity and population structure analysis of drought tolerance in walnut (*Juglans regia* L.) using SSR markers. Plant Mol. Biol. Rep. 44, 5.
Vahdati, K., Lotfi, N., Kholdebarin, B., Hassani, D., Amiri, R., Mozaffari, M.R., Leslie, C., 2009. Screening for drought-tolerant genotypes of Persian walnuts (*Juglans regia* L.) during seed germination. HortScience 44 (7), 1815–1819.
Vahdati, K., Arab, M.M., Sarikhani, S., Sadat-Hosseini, M., Leslie, C.A., Brown, P.J., 2019. Advances in persian walnut (*Juglans regia* L.) breeding strategies. In: Al-Khayri, J., Jain, S., Johnson, D. (Eds.), Advances in Plant Breeding Strategies: Nut and Beverage Crops. Springer, Cham.
Vahdati, K., Sarikhani, S., Arab, M.M., Leslie, C.A., Dandekar, A.M., Aletà, N., Bielsa, B., Gradziel, T.M., Montesinos, Á., Rubio-Cabetas, M.J., Sideli, G.M., Serdar, Ü., Akyüz, B., Beccaro, G.L., Donno, D., Rovira, M., Ferguson, L., Akbari, M., Sheikhi, A., Sestras, A.F., Kafkas, S., Paizila, A., Roozban, M.R., Kaur, A., Panta, S., Zhang, L., Sestras, R.E., Mehlenbacher, S., 2021. Advanced in rootstock breeding of nut trees: objectives and strategies. Plants 10, 2234.
Vahdati, K., Sheikhi, A., Arab, M.M., Sarikhani, S., Habibi, A., Ataee, H., 2023. Cultivars and genetic improvement. In: Mir, M.M., Rehman, M.U., Iqbal, U., Mir, S.A. (Eds.), Temperate Nuts. Springer, Singapore.
Virtanen, P., Gommers, R., Oliphant, T.E., Haberland, M., Reddy, T., Cournapeau, D., Burovski, E., Peterson, P., Weckesser, W., Bright, J., Van Der Walt, S.J., 2020. SciPy 1.0: fundamental algorithms for scientific computing in Python. Nat. Methods 17 (3), 261–272.
Wei, M., Wang, M., Jiang, W., Zhao, Z., Sun, X., Fang, Y., Ma, T., 2025. Comprehensive evaluation of twelve kiwifruit (*Actinidia*) varieties on the winemaking adaptability based on multi-criteria decision-making method. Food Chem. 477, 143512.
Xu, X., Zhang, H., Yue, J., Xie, T., Xu, Y., Tian, Y., 2018. Predicting shifts in the suitable climatic distribution of walnut (*Juglans regia* L.) in China: maximum entropy model paves the way to forest management. Forests 9 (3), 103.
Zhou, R., Kan, X., Chen, J., Hua, H., Li, Y., Ren, J., Feng, K., Liu, H., Deng, D., Yin, Z., 2019. Drought-induced changes in photosynthetic electron transport in maize probed by prompt fluorescence, delayed fluorescence, P700 and cyclic electron flow signals. Environ. Exp. Bot. 158, 51–62.
Zuo, G., Mei, W., Feng, N., Zheng, D., 2025. Photosynthetic performance index (PIabs) and malondialdehyde (MDA) content determine rice biomass under combined salt stress and prohexadione-calcium treatment. BMC Plant Biol. 25, 823.